TARGETING HUMAN TELOMERASE RNA VIA BIOCHEMICAL AND *IN VITRO* SELECTION METHODS

Thesis by

Christine Terumi Ueda

In Partial Fulfillment of the Requirements

for the Degree of

DOCTOR OF PHILOSOPHY

CALIFORNIA INSTITUTE OF TECHNOLOGY

Pasadena, California

2007

(Defended September 5, 2006)

ACKNOWLEDGEMENTS

I want to thank Professor Rich Roberts for being a supportive advisor who shared great ideas with me and helped me grow into a complete scientist. I appreciate my committee members, Professor Jackie Barton, Professor Peter Dervan, and Professor Ray Deshaies, for their continued support and wisdom. I would also like to thank my family, both here and in New York City, for getting me to and through Caltech. My parents, Hideki and Akemi Ueda, spared nothing for my education and development. I will be eternally grateful to them for letting me make the choices that have richly enhanced my life. My brother, Jason, has been one of my biggest supporters, and I have valued all of our long-distance calls. I want to thank all my labmates, especially Dr. Terry Takahashi, with whom I have worked very closely during my time at Caltech. He has been a good friend and an invaluable resource to me. I would also like to mention Dr. Bill Ja, who always has great experimental advice and played softball and cribbage with me. I want to thank Ryan Austin and Dr. Adam Frankel for wonderful conversations over coffee and muffins. Steve Millward, Anders Olson, Dr. Shelley Starck, Dr. Cindy Qi, Dr. Shuwei Li, and Dr. Tianbing Xia provided helpful discussion and experimental advice on my work. Dr. Peter Snow and Cheryl Chow were excellent collaborators, and I am grateful for the work they contributed to this thesis. I want to thank my dear Palm Street/Los Robles housemates, Dr. Wendy Bittner, Garrett Bittner, Dr. Dave Michalak, and Dr. Julie Fry. Finally, I want to thank Dr. Robert Dirks for being a wonderful person and fiancé. He has been a constant source of excellent ideas and support. I am truly lucky to have him in my life.

ABSTRACT

Telomerase is an enzyme responsible for the maintenance of eukaryotic chromosome ends. The two main components required for activity are a protein subunit, the human telomerase reverse transcriptase (hTERT), and an RNA subunit, the human telomerase RNA (hTR). While telomerase is not active in most normal human cells, roughly 85% to 90% of oncogenic cells display increased telomerase activity. An understanding of the biochemistry of telomerase will aid in the development of molecules that will lead to antitumor-specific therapies. The first part of the work presented here describes a biochemical analysis of an RNA-RNA interaction between two catalytically important domains of hTR. The interactions were characterized via mobility-shift assay, mutation analysis, and UV cross-linking experiments. The data argue for a revised model for the structure of hTR, and point to possible three-dimensional contacts present in the telomerase complex. The next part of this thesis describes an *in vitro* selection against the catalytically important RNA stem-loop P6.1 in hTR. The *in vitro* selection was performed using mRNA display, which allows us to isolate RNA-binding peptides from libraries containing trillions of unique sequences. Unexpectedly, the selected peptide binds with high affinity and specificity to the relatively rare dimeric form of the P6.1 stem-loop rather than the more abundant monomeric conformation. Characterization of this novel RNA-peptide interaction was performed via circular dichroism, steady-state fluorescence, mobility-shift assay, and surface plasmon resonance. The data highlight the power of mRNA display to isolate high affinity ligands from large libraries of molecules.

TABLE OF CONTENTS

Page

FIGURES AND TABLES

Page

ABBREVIATIONS

CR conserved region

DNA deoxyribonucleic acid

hTR human telomerase RNA

hTERT human telomerase reverse transcriptase

mRNA messenger RNA

qPCR quantitative PCR

RNA ribonucleic acid

tRNA transfer RNA

CHAPTER 1:

INTRODUCTION

Chapter 1

INTRODUCTION

1.1 Human Telomerase

Telomerase is a ribonucleoprotein enzyme that is responsible for the replication of telomeres at the ends of eukaryotic chromosomes (Cech 2000; Bryan and Cech 1999; Harley 2002; Collins and Mitchell 2002). In normal human cells there is little or no telomerase activity, whereas in 80% to 90% of tumor cells there is active enzyme (Neidle and Parkinson 2002). The importance of telomerase in cancer is highlighted by its role in the first reported oncogenic transformation of human cells caused by defined genetic changes (Hahn et al. 1999); expression of the human telomerase reverse transcriptase protein (hTERT) in combination with two oncogenes converts normal human cells to tumor cells. This and other work has led to the notion that inhibitors of telomerase may represent general antitumor therapeutics. The work in this thesis represents our progress in (1) understanding telomerase via a biochemical study of an important RNA-RNA interaction in telomerase and (2) performing *in vitro* selection against telomerase to isolate peptides that will lead to the development of anticancer therapies.

Human telomerase consists of two essential components, the telomerase RNA (hTR), which is present in all human cells and acts as a template, and the telomerase reverse transcriptase protein (hTERT), which is not generally present at detectable levels in quiescent cells (figure 1.1). Interactions involving telomerase are quite complex *in vivo*. The telomerase enzyme is minimally dimeric (Wenz et al. 2001; Beattie et al. 2001) and interacts with a

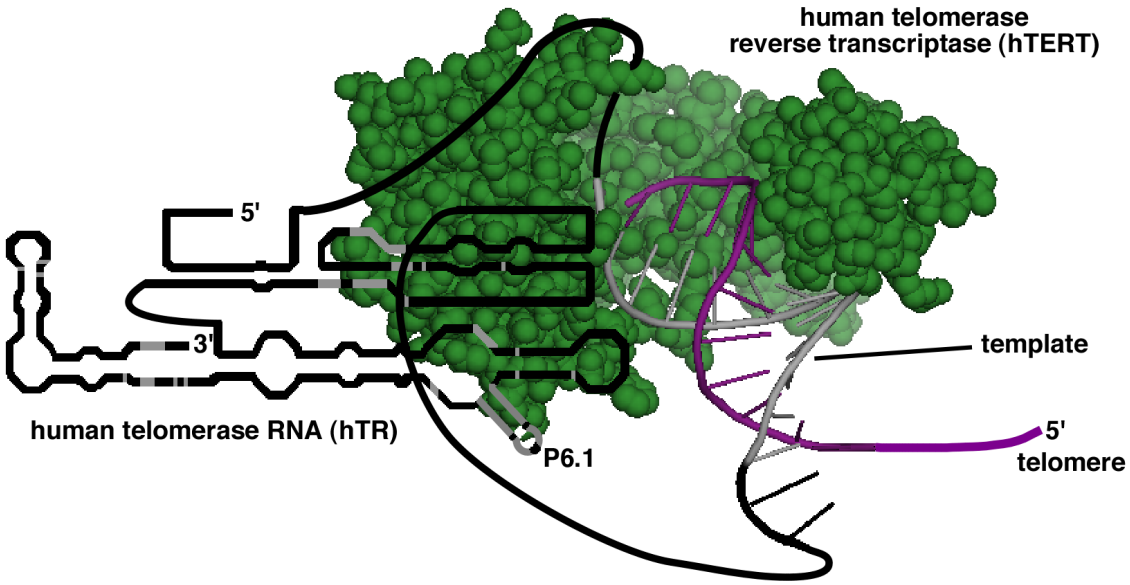

Figure 1.1. Model of the hTERT/hTR complex at the telomere (Lingner et al. 1997; Nakamura et al. 1997). The hTERT protein subunit (in green) is based on the crystal structure of the HIV-1 RT (Sarafianos et al. 1999). The hTR (in black and gray) is shown schematically in its secondary structure representation (adapted from Ueda and Roberts 2004). The template is shown in the active site of the reverse transcriptase, though the location of the rest of the RNA is unknown. Other associated proteins may be present in the complex, but are not shown.

complicated protein and nucleic acid architecture present at the ends of linear chromosomes (reviewed in Collins and Mitchell 2002; Blackburn 2001). A variety of factors, such as subcellular localization and the state of this complicated chromosome end structure, play roles in proper telomerase function. In order to study a complex as large as human telomerase, we have concentrated our efforts on the catalytically important regions of the hTR component. By targeting functionally important domains of hTR with an *in vitro* display strategy (e.g. mRNA display), we can isolate peptide ligands that have a high probability of affecting telomerase assembly and function.

Phylogenetic secondary structure analysis of telomerase RNA (Chen et al. 2000; figure 1.2), as well as characterization of hTR and hTERT deletion mutants (Autexier et al. 1996; Beattie et al. 1998; Tesmer et al. 1999; Mitchell and Collins 2000; Bachand and Autexier 2001; Bachand et al. 2001) highlight four conserved domains in the telomerase RNA: (1) the pseudoknot domain, (2) the box H/ACA, (3) the conserved region 4/5 (CR4/CR5), and (4) the conserved region 7 (CR7). Highly conserved portions of these domains (particularly CR4/CR5 and CR7) appear to be small, well-ordered RNA structures that could serve as excellent targets for selection experiments. Our effort to develop telomerase inhibitors should facilitate a mechanistic-biochemical understanding of this enzyme and its partners.

1.2 Telomerase Inhibition

Because regulation of telomerase represents an attractive target for antitumor-specific therapeutics, several laboratories have developed strategies for inhibiting telomerase (reviewed in Bearss et al. 2000; Shay 2005). One approach focuses on inducing and stabilizing G-quadruplex structures at the telomeres using small molecules (Sun et al. 1997; Harrison et al.

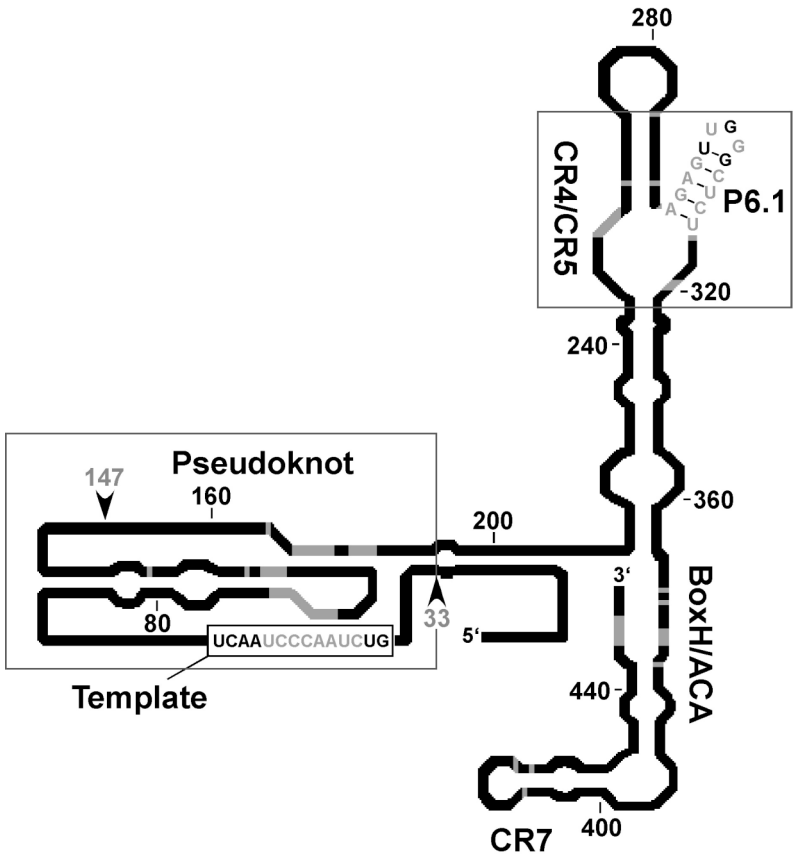

Figure 1.2. Secondary structure of hTR (adapted from Ueda and Roberts 2004). Gray bases indicate 100% conservation across all vertebrate telomerase RNAs. The domains essential for telomerase activity, the template, pseudoknot, and the CR4/CR5 domain are shown boxed. The catalytically critical P6.1 hairpin is also indicated. The box H/ACA and CR7 domains are important for hTR localization.

1999). Though this stabilization has been shown to inhibit telomerase as well as lead to telomere shortening and replicative senescence, G quadruplex structures are abundant in a variety of regions with nontelomere-related biological activities (reviewed in Davis 2004). Targeting the telomere-associated proteins, such as telomeric-repeat binding factor 1 (TRF1), also represents a promising approach to telomerase inhibition. By targeting tankyrase 1, Seimiya and co-workers caused an increase of TRF1 loading on the chromosome end, restricting access to the telomere, and reducing telomerase activity (2005). However, effective inhibition required use of a telomerase inhibitor in combination with the tankyrase 1 inhibitor.

Because hTERT is a reverse transcriptase, the effects of several reverse transcriptase inhibitors (RTIs) on telomerase have been investigated (Strahl and Blackburn 1996). However, out of the seven RTIs tested, only one nucleoside analog (ddG) consistently caused progressive telomere shortening in immortalized cell lines. This shortening, however, did not cause cellular senescence or any change in cell growth rates after one year of treatment. A second approach to targeting hTERT is via antisense oligonucleotides that are designed to hybridize to the hTERT mRNA, and deplete hTERT protein levels inside the cell. However, recent studies have shown that anti-hTR oligomers are more effective in blocking telomerase expression than strategies targeting hTERT mRNA (Natarajan et al. 2004).

Other methods for telomerase inhibition rely on base pairing to the telomerase RNA (hTR). These hTR binders include: (1) PNA molecules (Norton et al. 1996), (2) ribozymes (Wan et al. 1998), (3) 2'-deoxy and 2' substituted N3' → P5' phosphoramidate oligonucleotides, (4) N3' → P5' thio-phosphoramidate oligonucleotides (Asai et al. 2003; Akiyama et al. 2003; Herbert et al. 2005), and (5) oligonucleotides preventing proper assemblage of the

hTR/hTERT complex (Dominick et al. 2004). Many of these oligonucleotide hybridization molecules target the single-stranded templating region of hTR. They are necessarily sequence specific and therefore vulnerable to mutations in the sequence. The strategies described above represent much progress in the telomerase field, yet none of these inhibitors has proven efficacious in clinical trials.

A strategy focusing on ligands that are directed at structural elements in hTR may prove successful in developing novel, effective anticancer therapeutics. Up until now, groups have not targeted specific structural features of the hTR, but have rather focused on simple hybridization to the hTR sequence. In order to rationally design structure-based telomerase inhibitors, an accurate three-dimensional structure is critical. Only recently have groups been able to elucidate catalytically important elements in hTR by NMR, including the pseudoknot and two hairpins in the CR4/CR5 domain (Comolli et al. 2002; Theimer et al. 2003; Leeper et al. 2003; Leeper and Varani 2005). How these structural elements interact within the global context of the telomerase enzyme is still unknown, but with increased structural information, the structure-based rational design strategy may prove effective in developing telomerase inhibitors. In the meantime, targeting structural elements via *in vitro* selection presents a powerful tool to develop possible antitumor therapies.

We are focused on developing high affinity ligands that target a key structural element in the telomerase RNA, the P6.1 stem loop in the CR4/CR5 domain (figure 1.1; figure 1.2). Studies by Mitchell and Collins (2000) show that deletion of the region containing the P6.1 hairpin interferes with proper hTR and hTERT interaction, and abrogates telomerase activity. Additionally, mutation of the P6.1 loop causes loss of telomerase activity, highlighting the

importance of this hairpin in telomerase (Chen et al. 2002). The recent NMR structure of the stem loop from Leeper and co-workers shows that P6.1 is part of a well-defined structure that allows the exposed loop to participate in tertiary interactions with other portions of hTR, or in RNA-protein interactions with hTERT (2003). By targeting the P6.1, we hope to interfere with critical RNA-RNA or RNA-protein interactions and affect telomerase activity.

Though antisense approaches have had some success in targeting the hTR sequence, polypeptide ligands that target specific RNA structures provide an excellent alternative to oligonucleotide inhibitors for several reasons. First, our approach enables targeting folded RNA domains that are part of a larger complex, rather than simple, single-stranded regions. Our approach should therefore enable the development of inhibitors that are both highly specific and able to gain access to functionally critical regions, even in a very large functional RNA-protein complex. Second, peptides and peptide derivatives should have better bioavailability than oligonucleotides and their derivatives. Based on our experience, the RNA-binding peptides we develop will contain a number of basic (positively charged) residues that interact favorably with the negatively charged hTR RNA target. Positively charged RNA-binding peptides can often be engineered to cross cellular membranes and be transported to the nucleus (Schwarze et al. 2000; Derossi et al. 1998), while oligonucleotides have difficulty doing so unless modified to compensate for the negatively charged backbone. Alternatively, relatively hydrophobic peptides (e.g., cyclosporin) can show good oral bioavailability, have relatively long half-lives in humans, and can cross cellular membranes to act on their intracellular molecular targets (Christians and Sewing 1993; Fahr 1993; Hardman et al. 1996). Third, compared to oligonucleotides, peptides possess a more diverse set of chemical functionalities that likely make

them better candidates for medicinal chemistry and rational drug design development. Finally, inhibitors that recognize a key structural element may be more resistant to mutations than oligonucleotides. Mutations in the sequence that are able to preserve structure and function would likely disrupt the hybridization of oligonucleotide inhibitors, yielding them ineffective. However, changes in the RNA target that can simultaneously evade the peptide ligand and preserve telomerase function are expected to be very rare because if the structure of the RNA is retained, the structural recognition of the peptide ligand would also likely be preserved. These reasons make peptide-targeting of a critical structural element an attractive strategy for developing drugable inhibitors of telomerase function.

1.3 *In Vitro* Selection via mRNA Display

The mRNA display technique is a powerful tool used to perform *in vitro* selection of peptides using RNA-peptide fusions (Roberts and Szostak 1997; Roberts 1999; reviewed in Takahashi et al. 2003). In this approach, encoded peptide libraries are constructed as covalent fusions with their own mRNA (figure 1.3). The sequence present in the peptide is then encoded in the covalently attached mRNA, allowing the sequence information in the peptide to be read and recovered via the attached RNA. The mRNA display system has been extensively optimized, particularly for the development of RNA-binding ligands (Liu et al. 2000; figure 1.4). This work has resulted in the ability to perform selection experiments on peptide libraries containing trillions of molecules (Cho et al. 2000; Keefe and Szostak 2001; Wilson et al. 2001; Barrick et al. 2001b). Compared with other functional approaches, the mRNA display system allows libraries with approximately 10^4-fold more sequence complexity than phage display (Smith and Petrenko 1997), 10^6-fold more than yeast display or yeast two- and three-hybrid

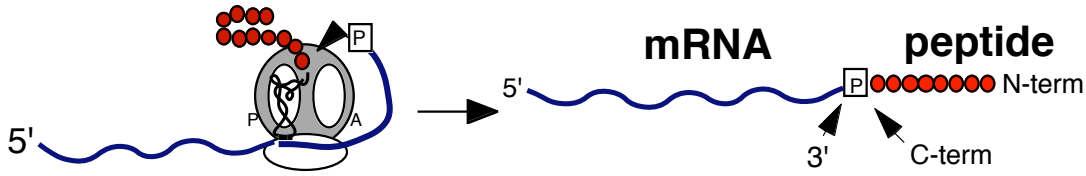

Figure 1.3. Formation of an mRNA-peptide fusion using *in vitro* translation of 3' puromycin templates (adapted from Roberts 1999). The mRNA (in blue) is covalently linked to the peptide (in red) it encodes for via the 3' puromycin (indicated by the boxed P).

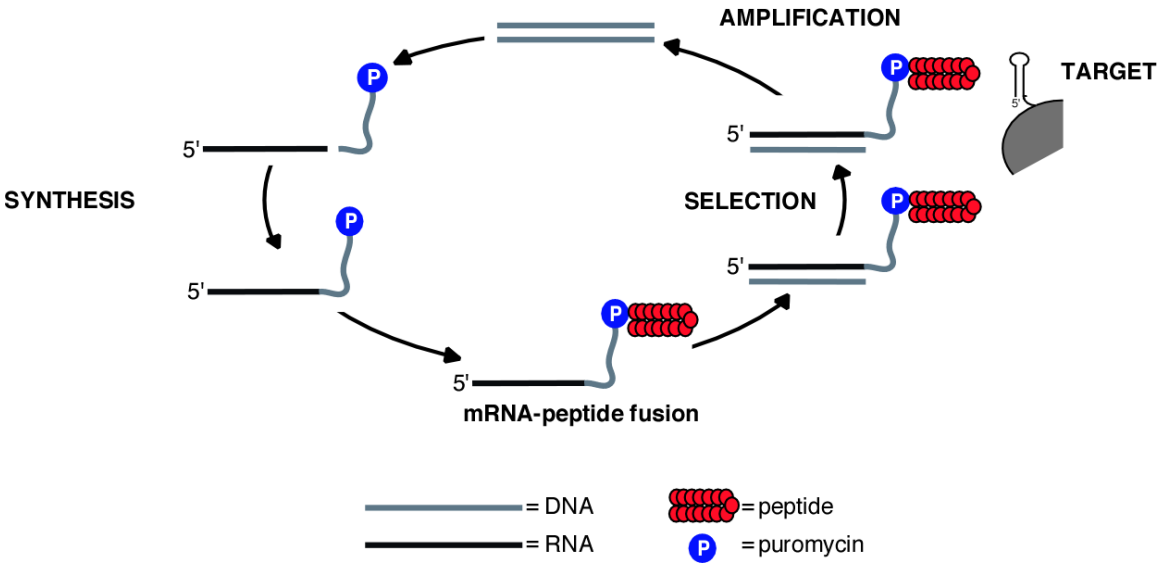

Figure 1.4. Optimized selection cycle (adapted from Roberts 1999). The library is first synthesized to produce mRNA-peptide fusions, then passed over an immobilized target during the selection step, and finally amplified in order to start the next round of synthesis.

systems (Fields and Song, 1989; Gyuris et al. 1993; Sengupta et al. 1996; Boder and Wittrup 1997), and approximately 10^9-fold more than colony screening approaches (Arnold and Volkov 1999).

Our laboratory has designed high affinity, high specificity peptides that bind to structured RNA elements (Barrick et al. 2001a, 2001b; Austin et al. 2002; Xia et al. 2003). We have examined libraries ranging from 20 sequences to more than 9 trillion individual members using the *in vitro* selection cycle (figure 1.4). This work has led to the development of diverse, structure-specific, high affinity peptide ligands. Primary selection experiments have typically resulted in molecules that bind with low nanomolar affinity (Barrick et al. 2001b). *In vitro* evolution experiments, negative selection steps, mutagenic PCR (Beaudry and Joyce 1992; Cadwell and Joyce 1992), mutational analysis, and sequence covariation (Barrick and Roberts 2002) can enable the design of very high affinity molecules that bind into the low picomolar range, tighter than many macromolecular RNA-protein and protein-protein interactions.

1.4 Thesis Overview

Understanding telomerase structure and function is essential to developing effective anticancer therapeutics via telomerase inhibition. Toward that end, a biochemical study of the interactions between two regions of the human telomerase RNA critical for telomerase activity (chapter 2), and an *in vitro* selection against a catalytically important structural element of hTR (chapter 3) were carried out and are presented in this thesis.

Chapter 2 describes a published biochemical study of a long-range RNA-RNA interaction between conserved domains in human telomerase RNA. The catalytically critical stem-loop P6.1 can participate in an RNA-RNA interaction with the template region of hTR.

The data argue for the close proximity of the template and the CR4/CR5 domain in three-dimensional space, and provide the basis for a revised model of hTR, partitioning the RNA into a catalytic domain and a localization domain.

Chapter 3 describes an *in vitro* selection performed against the P6.1 hairpin element in hTR via mRNA display. The selected peptide is characterized biochemically and biophysically utilizing steady-state fluorescence, circular dichroism, surface plasmon resonance, and mobility-shift assay. Unexpectedly, the peptide does not bind the monomeric P6.1 hairpin, but instead binds to the less abundant dimeric form with 130 pM affinity at 37 °C in 150 mM monovalent salt; this association is among the tightest known peptide-RNA interactions. The structure in the core of the P6.1 dimer RNA contains a G-G bulge flanked by four G-U wobble base pairs, which represents a novel peptide recognition site. This selection underscores the need to carefully evaluate the choice and design of targets for *in vitro* selection experiments, and highlights the ability of mRNA display to select for peptides with high specificity and affinity for RNA targets.

Appendix A details work accomplished toward developing methods to study the changing population between rounds of selection as well as monitor the progress of a selection via quantitative PCR. Appendix B explains efforts to redesign the P6.1 target, and modify the protocols for selection against the new P6.1 hairpin target. Appendix C describes the expression and mobility-shift analysis of the RNA-binding domain of the hTERT component of the telomerase complex.

Bibliography

Akiyama, M., T. Hideshima, M. A. Shammas, T. Hayashi, M. Hamasaki, Y. T. Tai, P. Richardson, S. Gryaznov, N. C. Munshi, and K. C. Anderson. 2003. Effects of oligonucleotide N3'→P5' thio-phosphoramidate (GRN163) targeting telomerase RNA in human multiple myeloma cells. *Cancer Res.* **63**: 6187-6194.

Arnold, F. H. and A. A. Volkov. 1999. Directed evolution of biocatalysts. *Curr. Opin. Chem. Biol.* **3**: 54-59.

Asai, A., Y. Oshima, Y. Yamamoto, T. A. Uochi, H. Kusaka, S. Akinaga, Y. Yamashita, K. Pongracz, R. Pruzan, E. Wunder, M. Piatyszek, S. Li, A. C. Chin, C. B. Harley, and S. Gryaznov. 2003. A novel telomerase template antagonist (GRN163) as a potential anticancer agent. *Cancer Res.* **63**: 3931-3939.

Austin, R. J., T. Xia, J. Ren, T. T. Takahashi, R. W. and Roberts. 2002. Designed arginine-rich RNA-binding peptides with picomolar affinity. *JACS* **124**: 10966-10967.

Autexier, C., R. Pruzan, W. D. Funk, and C. W. Greider. 1996. Reconstitution of human telomerase activity and identification of a minimal functional region of the human telomerase RNA. *EMBO J.* **15**: 5928-5935.

Bachand, F. and C. Autexier. 2001. Functional regions of human telomerase reverse transcriptase and human telomerase RNA required for telomerase activity and RNA-protein interactions. *Mol. Cell Biol.* **21**: 1888-1897.

Bachand, F., I. Triki, and C. Autexier. 2001. Human telomerase RNA-protein interactions. *Nuc. Acids Res.* **29**: 3385-3393.

Barrick, J. E. and R. W. Roberts. 2002. Sequence analysis of an artificial family of RNA-binding peptides. *Prot. Sci.* **11**: 2688-2696.

Barrick, J. E., T. T. Takahashi, A. Balakin, and R. W. Roberts. 2001a. Selection of RNA-binding peptides using mRNA-peptide fusions. *Methods* **23**: 287-293.

Barrick, J. E., T. T. Takahashi, J. Ren, T. Xia, and R. W. Roberts. 2001b. Large libraries reveal diverse solutions to an RNA recognition problem. *Proc. Natl. Acad. Sci. USA* **98**: 12374-12378.

Bearss, D. J., L. H. Hurley, and D. D. Von Hoff. 2000. Telomere maintenance mechanisms as a target for drug development. *Oncogene.* **19:** 6632-6641.

Beattie, T. L., W. Zhou, M. O. Robinson, and L. Harrington. 1998. Reconstitution of human telomerase activity *in vitro*. *Curr. Biol.* **8**: 177-180.

Beattie, T. L., W. Zhou, M. O. Robinson, and L. Harrington. 2001. Functional multimerization of the human telomerase reverse transcriptase. *Mol. Cell. Biol.* **21**: 6151-6160.

Beaudry, A. A. and G. F. Joyce. 1992. Directed evolution of an RNA enzyme. *Science* **257**: 635-641.

Blackburn, E. H. 2001. Switching and signaling at the telomere. *Cell* **106**: 661-673.

Boder, E. T. and K. D. Wittrup. 1997. Yeast surface display for screening combinatorial polypeptide libraries. *Nat. Biotechnol.* **15**:553-557.

Bryan, T. M. and T. R. Cech. 1999. Telomerase and the maintenance of chromosome ends. *Curr. Opin. Cell Biol.* **11**: 318-324.

Cadwell, R. C. and G. F. Joyce. 1992. Randomization of genes by PCR mutagenesis. *PCR Methods Appl.* **2**: 28-33.

Cech, T. R. 2000. Life at the end of the chromosome: Telomeres and telomerase. *Angew. Chem. Int. Ed.* **39**: 34-43.

Chen, J. L., M. A. Blasco, and C. W. Greider. 2000. Secondary structure of vertebrate telomerase RNA. *Cell* **100**: 503-514.

Chen, J. L., K. K. Opperman, and C. W. Greider. 2002. A critical stem-loop structure in the CR4-CR5 domain of mammalian telomerase RNA. *Nuc. Acids Res.* **30**: 592-597.

Cho, G., A. D. Keefe, R. Liu, D. S. Wilson, and J. W. Szostak. 2000. Constructing high complexity synthetic libraries of long ORFs using *in vitro* selection. *J. Mol. Biol.* **297**: 309-319.

Christians, U. and K. F. Sewing. 1993. Cyclosporin metabolism in transplant patients. *Pharmacol. Ther.* **57**: 291-345.

Collins, K. and J. R. Mitchell. 2002. Telomerase in the human organism. *Oncogene* **21**: 564-579.

Comolli, L. R., I. Smirnov, L. Xu, E. H. Blackburn, and T. L. James. 2002. A molecular switch underlies a human telomerase disease. *Proc. Natl. Acad. Sci. USA* **99**: 16998-17003.

Davis, J. T. 2004. G-quartets 40 years later: From 5'-GMP to molecular biology and supramolecular chemistry. *Angew. Chem. Int. Ed.* **43**: 668-698.

Derossi, D., G. Chassaing, and A. Prochiantz. 1998. Trojan peptides: The penetratin system for intracellular delivery. *Trends Cell Biol.* **8**: 84-87.

Dominick, P. K., B. R. Keppler, J. D. Legassie, I. K. Moon, and M. B. Jarstfer. 2004. Nucleic acid-binding ligands identify new mechanisms to inhibit telomerase. *Bioorg. Med. Chem. Lett.* **14**: 34667-71.

Fahr, A., 1993. Cyclosporin clinical pharmacokinetics. *Clin. Pharmacokinet.* **24**: 472-495.

Fields, S. and O. Song. 1989. A novel genetic system to detect protein-protein interactions. *Nature* **340**: 245-246.

Gyuris, J., E. Golemis, H. Chertokov, and R. Brent. 1993. Cdi1, a human G1 and S phase protein phosphatase that associates with Cdk2. *Cell* **75**: 791-803.

Hahn, W. C., C. M. Counter, A. S. Lundberg, R. L. Beijersbergen, M. W. Brooks, and R. A. Weinberg. 1999. Creation of human tumor cells with defined genetic elements. *Nature* **400**: 464-468.

Hardman, J. G., A. G. Gilman, and L. E. Limbird, eds. 1996. *Goodman and Gilman's The Pharmacological Basis of Therapeutics*. 9th ed. New York: McGraw-Hill. 1905.

Harley, C. B. 2002. Telomerase is not an oncogene. *Oncogene* **21**: 494-502.

Harrison, R. J., S. M. Gowan, L. R. Kelland, and S. Neidle. 1999. Human telomerase inhibition by substituted acridine derivatives. *Bioorg. Med. Chem. Lett.* **9**: 2463-2468.

Herbert, B. S., G. C. Gellert, A. Hochreiter, K. Pongracz, W. E. Wright, D. Zielinska, A. C. Chin, C. B. Harley, J. W. Shay, and S. M. Gryaznov. 2005. Lipid modification of GRN163, an N3'→P5' thio-phosphoramidate oligonucleotide, enhances the potency of telomerase inhibition. *Oncogene* **24**: 5262-5268.

Keefe, A. D. and J. W. Szostak. 2001. Functional proteins from a random-sequence library. *Nature* **410**: 715-718.

Leeper, T., N. Leulliot, and G. Varani. 2003. The solution structure of an essential stem-loop of human telomerase RNA. *Nuc. Acids Res.* **31**: 2614-2621.

Leeper, T. and G. Varani. 2005. The structure of an enzyme-activating fragment of human telomerase RNA. *RNA* **11**: 394-403.

Lingner, J., T. R. Hughes, A. Shevchenko, M. Mann, V. Lundblad, and T. R. Cech. 1997. Reverse transcriptase motifs in the catalytic subunit of telomerase. *Science* **276**: 561-567.

Liu, R., J. E. Barrick, J. W. Szostak, and R. W. Roberts. 2000. Optimized synthesis of RNA-protein fusions for *in vitro* protein selection. *Methods Enzymol.* **317**: 268-293.

Mitchell, J. R. and K. Collins. 2000. Human telomerase activation requires two independent interactions between telomerase RNA and telomerase reverse transcriptase. *Mol. Cell* **6**: 361-371.

Nakamura, T. M., G. B. Morin, K. B. Chapman, S. L. Weinrich, W. H. Andrews, J. Lingner, C. B. Harley, and T. R. Cech. 1997. Telomerase catalytic subunit homologs from fission yeast and human. *Science* **277**: 955-959.

Natarajan, S., Z. Chen, E. V. Wancewicz, B. P. Monia, and D. R. Corey. 2004. Telomerase reverse transcriptase (hTERT) mRNA and telomerase RNA (hTR) as targets for downregulation of telomerase activity. *Oligonucleotides* **14**: 263-273.

Neidle, S. and G. Parkinson. 2002. Telomere maintenance as a target for anticancer drug discovery. *Nature Reviews Drug Discovery* **1**: 383-393.

Norton, J. C., M. A. Piatyszek, W. E. Wright, J. W. Shay, and D. R. Corey. 1996. Inhibition of human telomerase activity by peptide nucleic acids. *Nat. Biotechnol.* **14**: 615-619.

Roberts, R. W. 1999. Totally *in vitro* protein selection using mRNA-protein fusions and ribosome display. *Curr. Opin. Chem. Biol.*, **3**: 268-273.

Roberts, R. W. and J. W. Szostak. 1997. RNA-peptide fusions for the *in vitro* selection of peptides and proteins. *Proc. Natl. Acad. Sci. USA* **94**: 12297-12302.

Sarafianos, S. G., K. Das, A. D. Clark Jr., J. Ding, P. L. Boyer, S. H. Hughes, and E. Arnold. 1999. Lamivudine (3TC) resistance in HIV-1 reverse transcriptase involves steric hindrance with beta-branched amino acids. *Proc. Natl. Acad. Sci. USA* **96**: 10027-10032.

Schwarze, S. R., K. A. Hruska, and S. F. Dowdy. 2000. Protein transduction: Unrestricted delivery into all cells? *Trends Cell Biol.* **10**: 290-295.

Seimiya, H., Y. Muramatsu, T. Ohishi, and T. Tsuruo. 2005. Tankyrase 1 as a target for telomere-directed molecular cancer therapeutics. *Cancer Cell* **7**: 25-37.

Sengupta, D. J., B. Zhang, B. Kraemer, P. Pochart, S. Fields, and M. Wickens. 1996. A three-hybrid system to detect RNA-protein interactions *in vivo*. *Proc. Natl. Acad. Sci. USA* **93**: 8496-8501.

Shay, J. W. 2005. Meeting report: The role of telomeres and telomerase in cancer. *Cancer Res.* **65**: 3513-3517.

Smith, G. P. and V. A. Petrenko. 1997. Phage display. *Chem. Rev.* **97**: 391-410.

Strahl, C. and E. H. Blackburn. 1996. Effects of reverse transcriptase inhibitors on telomere length and telomerase activity in two immortalized human cell lines. *Mol. Cell Biol.* **16**: 53-65.

Sun, D., B. Thompson, B. E. Cathers, M. Salazar, S. M. Kerwin, J. O. Trent, T. C. Jenkins, S. Neidle and L. H. Hurley. 1997. Inhibition of human telomerase by a G-quadruplex-interactive compound. *J. Med. Chem.* **40**: 2113-2116.

Takahashi, T. T., R. J. Austin, and R. W. Roberts. 2003. mRNA display: Ligand discovery, interaction, and beyond. *Trends Biochem. Sci.* **28**: 159-65.

Tesmer, V. M., L. P. Ford, S. E. Holt, B. C. Frank, X. Yi, D. L. Aisner, M. Ouellette, J. W. Shay, and W. E. Wright. 1999. Two inactive fragments of the integral RNA cooperate to assemble active telomerase with the human protein catalytic subunit (hTERT) *in vitro*. *Mol. Cell Biol.* **19**: 6207-6216.

Theimer, C. A., L. D. Finger, L. Trantirek, and J. Feigon. 2003. Mutations linked to dyskeratosis congenita cause changes in the structural equilibrium in telomerase RNA. *Proc. Natl. Acad. Sci. USA* **100**: 449-454.

Ueda, C. T. and R. W. Roberts. 2004. Analysis of a long-range interaction between conserved domains of human telomerase RNA. *RNA* **10**: 139-147.

Wan, M. S., P. L. Fell, and S. Akhtar. 1998. Synthetic 2'-O-methyl-modified hammerhead ribozymes targeted to the RNA component of telomerase as sequence-specific inhibitors of telomerase activity. *Antisense Nucleic Acid Drug Dev.* **8** 309-317.

Wenz, C., B. Enenkel, M. Amacker, C. Kelleher, K. Damm, and J. Lingner. 2001. Human telomerase contains two cooperating telomerase RNA molecules. *EMBO J.* **20**: 3526-3534.

Wilson, D. S., A. D. Keefe, and J. W. Szostak. 2001. The use of mRNA display to select high-affinity protein-binding peptides. *Proc. Natl. Acad. Sci. USA* **98**: 3750-3755.

Xia, T. A. Frankel, T. T. Takahashi, J. Ren, and R. W. Roberts. 2003. Context and conformation dictate function of a transcription antitermination switch. *Nat. Struct. Biol.* **10**: 812-819.

CHAPTER 2:

ANALYSIS OF A LONG-RANGE INTERACTION BETWEEN CONSERVED DOMAINS OF HUMAN TELOMERASE RNA

This chapter was taken largely from C. T. Ueda and R. W. Roberts. 2004. Analysis of a long-range interaction between conserved domains of human telomerase RNA. *RNA* **10**: 139-147. Reprinted with copyright permission.

Chapter 2

ANALYSIS OF A LONG-RANGE INTERACTION BETWEEN CONSERVED DOMAINS OF HUMAN TELOMERASE RNA

2.1 Abstract

Telomerase is a ribonucleoprotein complex responsible for maintaining telomere length of eukaryotic chromosomes. Human telomerase has two main components, the human telomerase reverse transcriptase (hTERT) and the human telomerase RNA (hTR). Two domains of hTR essential for telomerase activity are the template domain, composed of an 11-nucleotide templating and alignment sequence, and the CR4/CR5 domain. Highly conserved residues in the CR4/CR5 domain form the stem-loop P6.1, which is important for the assembly and activity of mammalian telomerase. Here, we have determined that stem-loop P6.1 can participate in a long range RNA-RNA interaction with the template region of hTR. We characterized this interaction through mobility-shift assays, mutation analysis, and UV cross-linking experiments. Mutation analysis revealed that the P6.1 loop nucleotides participate in the interaction with the template. The site of interaction at the template domain was determined via UV cross-linking experiments. These data show that an RNA-RNA interaction exists between two highly conserved regions of hTR that are critical for the higher order folding of telomerase RNA. This interaction argues for the close proximity of the template and the CR4/CR5 domain, and provides the basis for a revised model of hTR, partitioning the RNA into a catalytic domain and a localization domain.

2.2 Introduction

Telomeres, the protective termini of eukaryotic chromosomes, are composed of G/T rich sequences (TTAGGG in vertebrates) and their associated proteins (Blackburn 1991; reviewed in Cech 2000 and Blackburn 2000). Telomerase is a reverse transcriptase responsible for the synthesis and addition of telomeric repeats to chromosomal ends (Greider and Blackburn 1985). This ribonucleoprotein complex acts to balance the effects of natural chromosomal shortening that occurs through incomplete DNA replication. Though telomerase activity is not detectable in normal human cells, telomerase is active in roughly 85% to 90% of oncogenic cells (Kim et al. 1994). In 1999, Weinberg and co-workers showed that the oncogenic transformation of human cells required hTERT (Hahn et al. 1999). These observations have led researchers to believe that telomerase is a promising target for the development of anticancer therapies (Corey 2002; Rezler et al. 2002).

The two main components of telomerase are the protein (TERT) and the RNA (TR). Telomerase reverse transcriptase (TERT) contains reverse transcriptase motifs essential for enzymatic activity as well as a telomerase specific T motif (Lingner et al. 1997; Nakamura et al. 1997). The stable association of TERT with a telomerase RNA containing the template for telomeric repeat synthesis is a unique feature of the telomerase reverse transcriptase (Greider and Blackburn 1989). Vertebrate telomerase RNA varies significantly in sequence and length (Chen et al. 2000). However, phylogenetic and covariation analysis of 35 vertebrate telomerase RNAs revealed that vertebrate telomerase RNAs share a similar secondary structure composed of highly conserved domains. The four conserved domains found in vertebrate telomerase

RNAs, including hTR are (1) the pseudoknot domain, (2) the box H/ACA domain, (3) the CR4/CR5 domain, and (4) the CR7 domain (Chen et al. 2000; figure 2.1).

Human telomerase RNA (hTR) is a 451-nucleotide RNA containing an 11-nucleotide templating region (5'-CUAACCC*UAAC*-3') located near its 5' terminus. The templating region is composed of the template sequence for the synthesis of d(GGTTAG) as well as an alignment domain (italicized) (Feng et al. 1995; Gavory et al. 2002). It has been proposed that the alignment domain hybridizes to the 3' terminus of the DNA substrate, and positions the telomere for processive synthesis of telomeric repeats (Greider and Blackburn 1989; Shippen-Lentz and Blackburn 1990; Autexier and Greider 1994).

The structurally conserved domains in hTR have specific functions in active telomerase. The box H/ACA and CR7 domains are dispensable for reconstitution of telomerase activity *in vitro* (Bachand and Autexier 2001). However, *in vivo*, the box H/ACA motif is required for the 3' terminal formation of the mature telomerase RNA (Mitchell et al. 1999). Additionally, the box H/ACA and CR7 domains participate in nucleolar localization of telomerase RNA (Lukowiak et al. 2001). It has been shown that the CR4/CR5 and pseudoknot domains are essential for catalytic activity (Tesmer et al. 1999; Beattie et al. 2000; Mitchell and Collins 2000; Martín-Rivera and Blasco 2001). *In vitro* studies indicate that these two domains can reconstitute telomerase activity in the presence of the protein component (Tesmer et al. 1999). Further studies have indicated that nucleotides 33-147 and 163-330 contain hTERT binding sites critical for telomerase activity (Bachand and Autexier 2001). Based on this evidence, we reasoned that RNA-RNA interactions, possibly critical for telomerase function, might be present in hTR involving these two conserved domains.

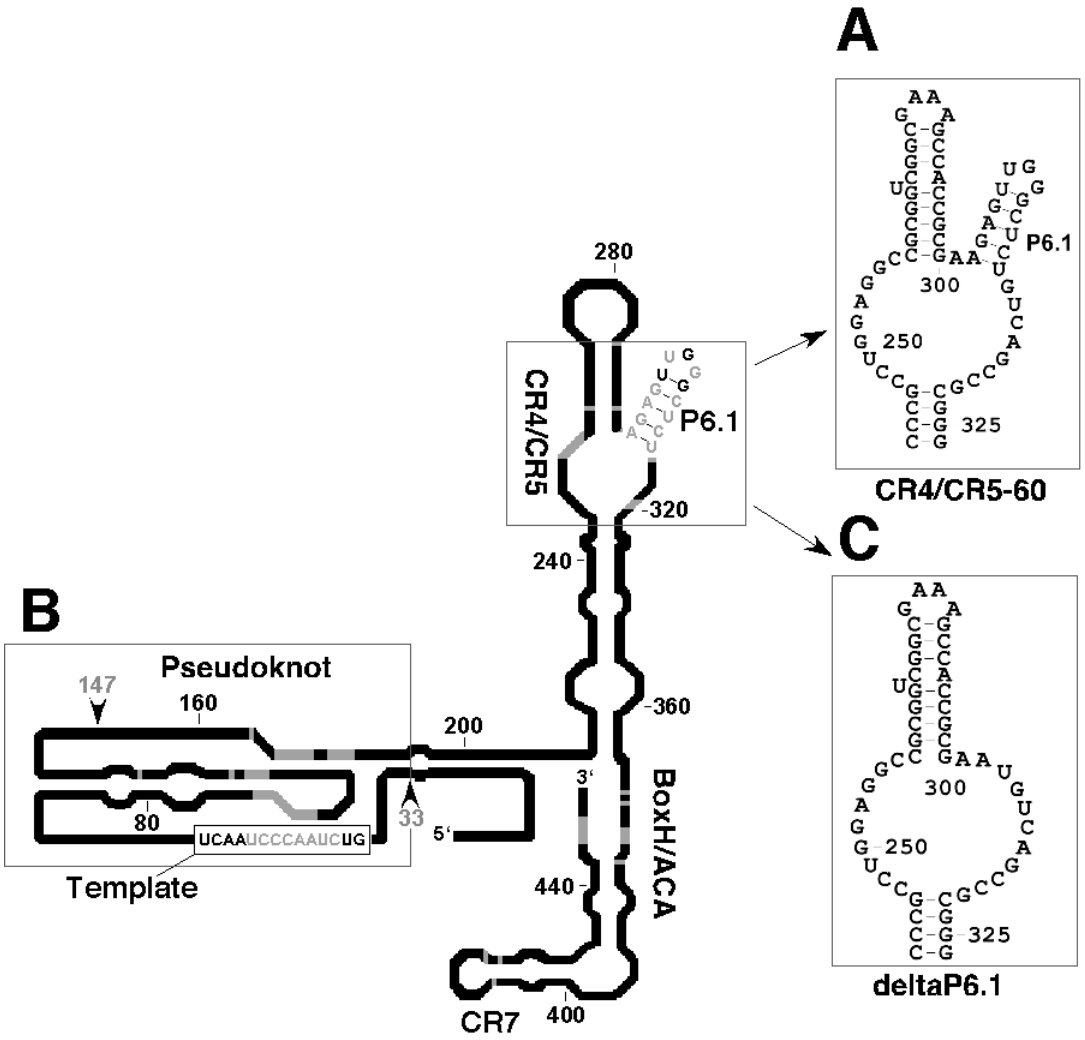

Figure 2.1. Human telomerase RNA constructs utilized to demonstrate RNA-RNA interactions via mobility-shift assays. The secondary structure of human telomerase RNA is adapted from Chen et al. (2000) with the following RNA regions indicated: (A) CR4/5-60, (B) RNA33-147 and (C) deltaP6.1. Bases in gray are 100% conserved in vertebrate telomerase RNA.

The data presented here show that an RNA-RNA interaction can exist between two hTR domains distant in primary sequence. We utilized separate domains of hTR in our structural characterization of the RNA. Gel mobility-shift assays, mutation analysis, and UV cross-linking identified the interacting residues as the P6.1 stem-loop in the CR4/CR5 domain and the template domain. Previous studies (Mitchell and Collins 2000; Chen et al. 2002) have indicated that P6.1 is a functionally important stem-loop in the CR4/CR5 domain in mammalian telomerase RNA. Recent NMR data from Varani and co-workers indicates that formation of P6.1 positions the exposed loop bases for possible RNA-RNA or RNA-protein interactions (Leeper et al. 2003). Our findings show that P6.1 participates in a long-range RNA-RNA interaction with residues in the template region of hTR. Because the regions participating in this interaction are highly conserved, this interaction may play a critical role in the catalytic activity of the telomerase complex.

2.3 Results

2.3.1 hTR RNA-RNA interaction revealed by mobility-shift assay

Because the pseudoknot and the CR4/CR5 domains have been implicated in the catalytic activity of telomerase, we examined the possible existence of a long-range RNA-RNA interaction between these two highly conserved domains. RNA constructs containing the two domains were synthesized *in vitro* for use in RNA-RNA mobility-shift assays. CR4/5-60 contains the CR4/CR5 domain (nucleotides 243-326, hTR numbering) with the L6 loop (nucleotides 266-291) mutated to a GAAA tetraloop (figure 2.1A). RNA33-147 is composed of the template region and two strands of the pseudoknot domain (figure 2.1B).

In mobility-shift experiments, we find that RNA33-147 forms complex with CR4/5-60 (figure 2.2). When RNA33-147 is ^{32}P 5'-end labeled and in the presence of excess CR4/5-60 a slower migrating band, indicating occurrence of an RNA-RNA interaction, is observed (figure 2.2A). To confirm that RNA33-147 and CR4/5-60 interact, we performed the complementary experiment in which CR4/5-60 is radioactively labeled and in the presence of excess RNA33-147 (figure 2.2B). Our results indicate that these two distal domains within hTR can form a gel-stable RNA-RNA interaction.

We performed the interaction assays under both low (0.1 mM) and high (5 mM) magnesium ion concentrations to examine the magnesium dependence of the interaction. We find that band shifts do not depend significantly on the magnesium concentration in the binding buffer. However, the ability to detect RNA-RNA interactions does depend on the presence of 5 mM $MgCl_2$ in the gel and the gel running buffer. When the preformed complexes are run on a native gel in 1X TBE (90 mM Tris-borate, 2 mM EDTA), a shift is no longer observed due to the magnesium ion dependent nature of the interaction (data not shown). The mobility-shift gels contained in this study show discrete bands indicating that the RNA constructs and the complexes formed between them are stable under native conditions.

2.3.2 Identifying the site of interaction in the CR4/CR5 domain

We were next interested in defining the nucleotides within the CR4/CR5 domain that participate in the long-range interaction. Nucleotides 302-314 form the stem-loop P6.1 within the CR4/CR5 domain (figure 2.1). According to covariation analysis, these residues are highly conserved. Additionally, in mouse telomerase RNA, formation of this stem-loop was found to be important for catalytic activity (Chen et al. 2002). We examined the possibility that this

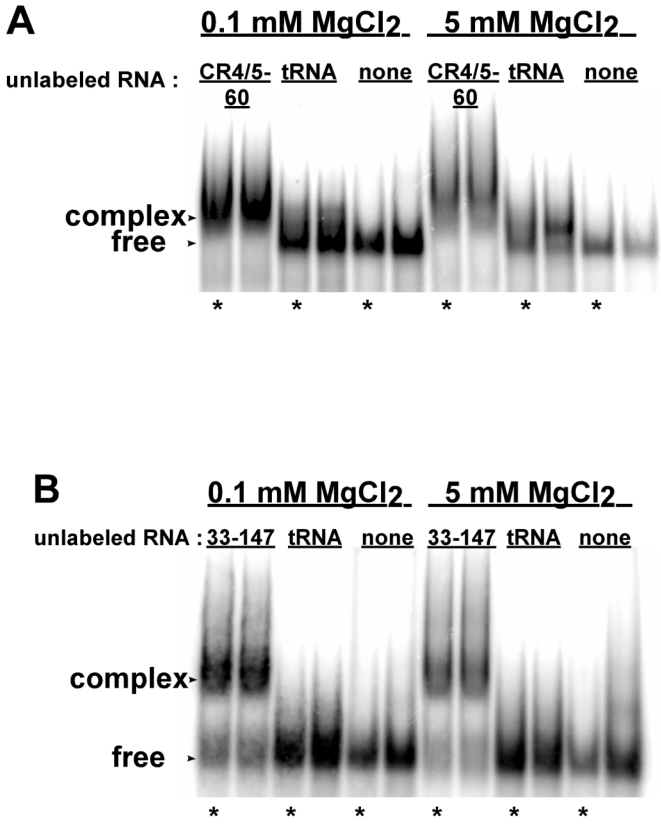

Figure 2.2. Native gel mobility-shift assays reveal complex formation between CR4/5-60 and RNA33-147. (A) ^{32}P 5'-end labeled RNA33-147 in the presence of excess unlabeled RNA. (B) ^{32}P 5'-end labeled CR4/5-60 in the presence of excess unlabeled RNA. For both (A) and (B), the indicated $MgCl_2$ concentrations correspond to $MgCl_2$ binding buffer concentrations (see section 2.5). Since minimal differences are observed between the two binding buffers, all following gels show samples assayed in 5 mM $MgCl_2$. Bands with reduced mobility in each gel correspond to an RNA-RNA complex while the faster migrating bands correspond to free RNA. Samples in lanes marked by a " * " (in this and all following mobility-shift gels) were incubated at 37 °C for 30 minutes prior to loading on 6% native gels.

stem-loop participates in the RNA-RNA interaction observed between the larger domain constructs. The P6.1 hairpin construct (figure 2.3A) was synthesized and used in a mobility-shift assay with RNA33-147 (figure 2.4A). The P6.1 band is shifted in the presence of RNA33-147. We used a competition mobility-shift assay between P6.1 and CR4/5-60 to determine if the two RNAs bind the template in the same manner (figure 2.4B). P6.1 does effectively compete with CR4/5-60 for the template, indicating that the smaller hairpin construct and the larger domain construct interact similarly with the template. A CR4/5-60 variant with P6.1 deleted (deltaP6.1; figure 2.1C) does not form complex with RNA33-147 (figure 2.5) indicating that this stem-loop is essential for the RNA-RNA interaction and confirming that P6.1 is the site of interaction. In mobility-shift assays, we determined that the K_d of RNA33-147 and P6.1 association is roughly 4 μM (data not shown).

Variants of the P6.1 hairpin were synthesized with mutations at the 7, 8, 9, and 10 positions indicated in figure 2.3A. According to covariation analysis (Chen et al. 2000), residues 8 and 10 are 100% conserved in vertebrate telomerase RNAs while residues 7 and 9 are variable across the different species. We therefore constructed the following individual mutants to determine which bases in the loop are essential for the RNA-RNA interaction: (1) U8C, (2) G10A, (3) G10C, (4) U7C, and (5) G9C. U8C, G10A, and G10C do not produce appreciable shifts (figure 2.6A-C). This result was expected since the U8 and G10 positions are 100% conserved and interfering with highly conserved residues is likely to disrupt the higher order structural interactions. U7C and G9C are able to interact with RNA33-147, though the amount of stable complex is reduced in comparison to that produced with wild-type hairpin. The more conservative U7C mutation leads to partial interaction while the less

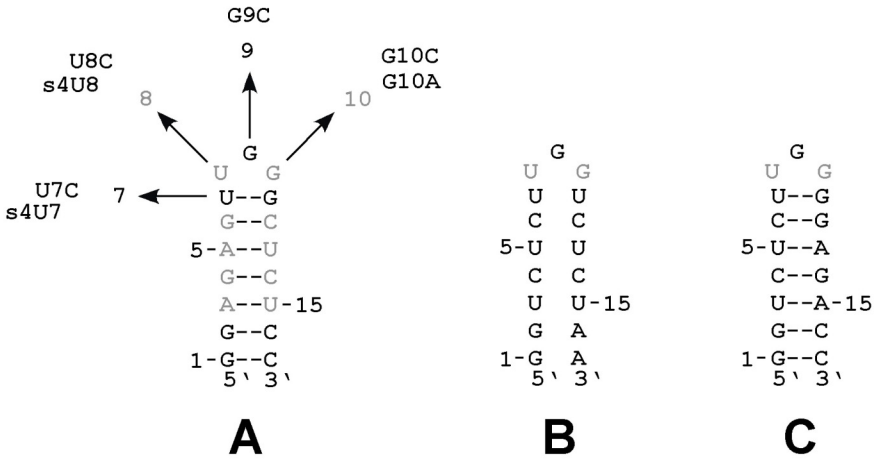

Figure 2.3. Secondary structure and mutation constructs of the P6.1 hairpin. Numbering corresponds to the nucleotide position in the hairpin beginning at the 5' end. Gray bases are 100% conserved in vertebrate telomerase RNAs (Chen et al. 2000). Hairpin A is wild-type P6.1 with the indicated mutations U7C, U8C, G9C, G10C, and G10A. UV cross-linking employed 4-thio-U modified RNA hairpins (designated as s4U7 and s4U8). Base-pairing in the stem of hairpin B is disrupted while the loop bases remained unchanged. Hairpin C restores base-pairing in the stem with an altered stem sequence.

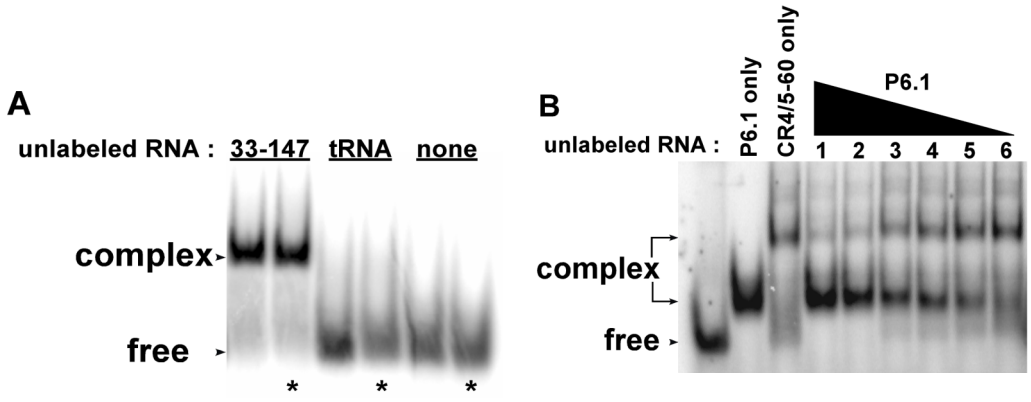

Figure 2.4. P6.1, a small hairpin located in the CR4/CR5 domain, participates in an RNA-RNA interaction with RNA33-147. (A) The P6.1 hairpin is ^{32}P 5'-end labeled and shifted with excess unlabeled RNA. (B) P6.1 and CR4/5-60 interact similarly with the template. The starting complex contains ^{32}P 5'-end labeled RNA44-57 in the presence of excess CR4/5-60 (10 μM). Lanes 1-6 contain the starting complex and decreasing amounts of P6.1 in the following concentrations: (1) 10 μM, (2) 5 μM, (3) 2 μM, (4) 1 μM, (5) 500 nM, and (6) 100 nM.

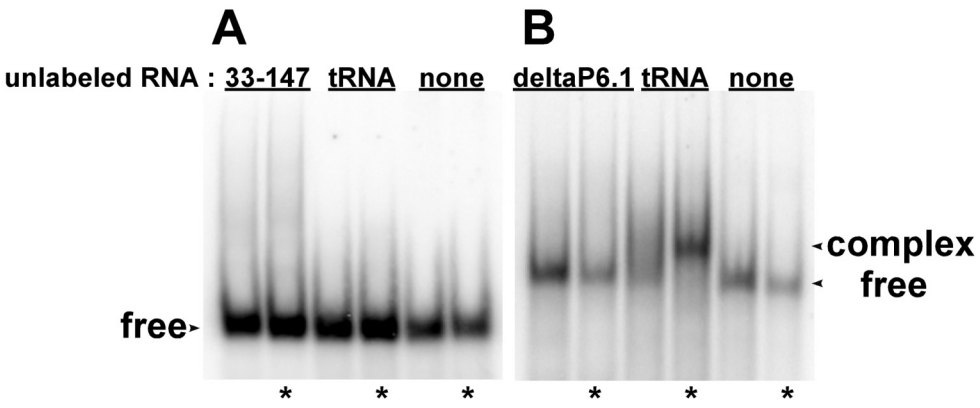

Figure 2.5. Deletion of the P6.1 stem-loop abrogates association of the mutant CR4/5-60 with RNA33-147. (A) ^{32}P 5'-end labeled deltaP6.1 in the presence of excess unlabeled RNA. (B) ^{32}P 5'-end labeled RNA33-147 in the presence of excess unlabeled RNA. The data show that no shift is observed when the P6.1 hairpin is deleted from the CR4/CR5 domain.

conservative mutation G9C results in lower binding affinity. Though U7 and G9 are not 100% conserved, mutation of U7 likely introduces a structural change in P6.1 leading to weaker RNA-RNA interaction. Mutation of G9 likely disrupts the interaction because it lies directly in the center of the loop, occupying an important point of contact. These mutation results indicate that the loop residues (5'-UGG-3') are necessary for the RNA-RNA interaction.

P6.1 stem mutants (figure 2.3B and C) were also utilized in mobility-shift assays. Formation of a stem of correct length is important for telomerase activity (Chen et al. 2002). The following stems were assayed: a P6.1 mutant that does not form a stem (figure 2.3B) and a P6.1 with a mutant stem (figure 2.3C; figure 2.6D). The P6.1 mutant that does not form a stem is unable to produce a shift in the presence of the template. The P6.1 with a mutant stem is able to interact with the template indicating that while the formation of the stem is required, the sequence of the stem can be variable. These data show that the P6.1 loop sequence as well as the formation of the stem are essential for the long-range interaction.

2.3.3 Defining the site of interaction in RNA33-147

We next investigated what positions within RNA33-147 are participating in the RNA-RNA interaction. To do this, we employed 4-thiouracil (4-thio-U) cross-linking, which would elucidate which bases within RNA33-147 are in close enough proximity to the loop region of the P6.1 hairpin to form cross-links. Two modified RNAs were synthesized; one contained a 4-thio-U modification at the U7 position (s4U7) while the other contained a 4-thio-U modification at the U8 position (s4U8) (figure 2.3A). Gel shift analysis shows that the 4-thio-U modified P6.1 constructs give comparable band shifts with RNA33-147 (data not shown).

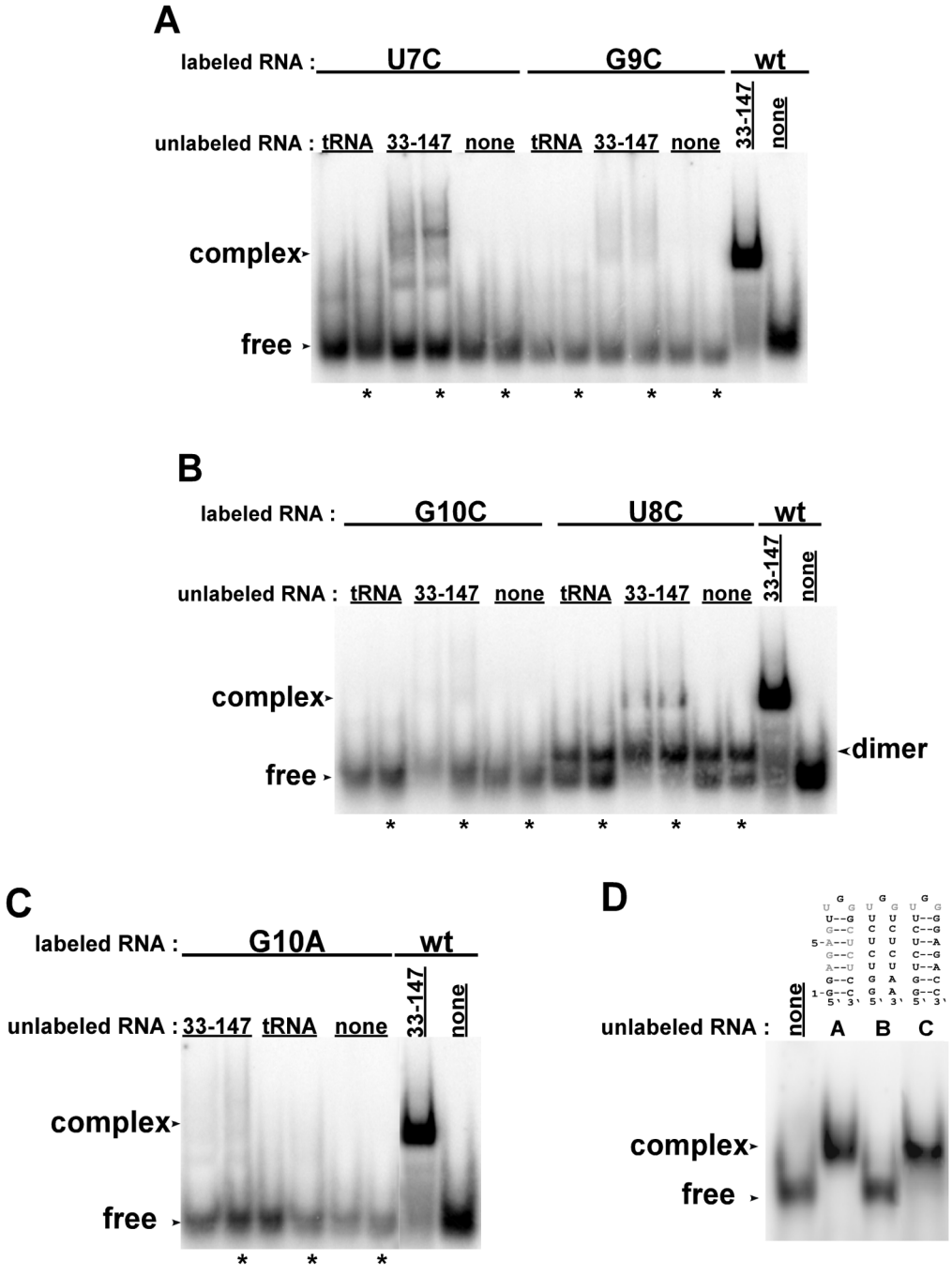

Figure 2.6. Mutation of the P6.1 hairpin loop sequence interferes with RNA complex formation between P6.1 and RNA33-147. (A) U7C and G9C introduce mutations at bases not 100% conserved across vertebrate telomerase RNAs (Chen et al. 2000). RNA complex

formation is observed, but at levels much lower than with wild-type P6.1 (wt) indicating that the interaction is much weaker in the presence of the mutated hairpin. (B) G10C and U8C introduce mutations at 100% conserved bases and also show greatly reduced complex formation. The hairpin with mutation U8C dimerizes under non-denaturing conditions, indicated by the bands with mobility between the free RNA and the complexed RNAs. (C) Mutation at P6.1 position G10 disrupts formation of the RNA-RNA complex.

Sequencing of the cross-linked products showed that the site of interaction within RNA33-147 occurs near the template sequence of hTR (figure 2.7). In the s4U7 experiments, the cross-linking occurs at positions G44, U45, and C46. In the s4U8 cross-linking experiment, the cross-linking occurs at A55.

To further verify the site of interaction, mobility-shift experiments were employed with small RNA fragments from the RNA33-67 region (figure 2.8). Initially, RNA33-147 was reduced to RNA33-67 to determine if the RNA-RNA interaction could be detected in the absence of any part of the pseudoknot. RNA33-67, encompassing only bases 5' of the pseudoknot region, shifts the P6.1 hairpin (figure 2.8). To further isolate the site of interaction, three short RNA fragments were synthesized: (1) RNA33-51, (2) RNA44-57, and (3) RNA52-67 (figure 2.8A). Two of the RNAs, RNA33-51 and RNA52-67, contain only a portion of the template region, while the third, RNA44-57, contains the entire template region. Only RNA44-57 shifts P6.1, indicating that the entire template is necessary for interaction with the hairpin (figure 2.8B). A further truncation of RNA44-57, involving only the 11- nucleotide templating domain, 5'- CUAACCCUAAC-3', shifts the P6.1 hairpin (figure 2.9). In a competition assay, we show that tRNA (at concentrations of either 50 μg/mL or 250 μg/mL) cannot compete with P6.1 for binding of the template (figure 2.9). This result argues for the specificity of the interaction revealed in this study.

2.4 Discussion

The studies presented here argue for a new model of telomerase RNA architecture that involves higher order folding of hTR (figure 2.10). We propose that the CR4/CR5 and pseudoknot domains are close in space, though distal in primary sequence. Our data argue for

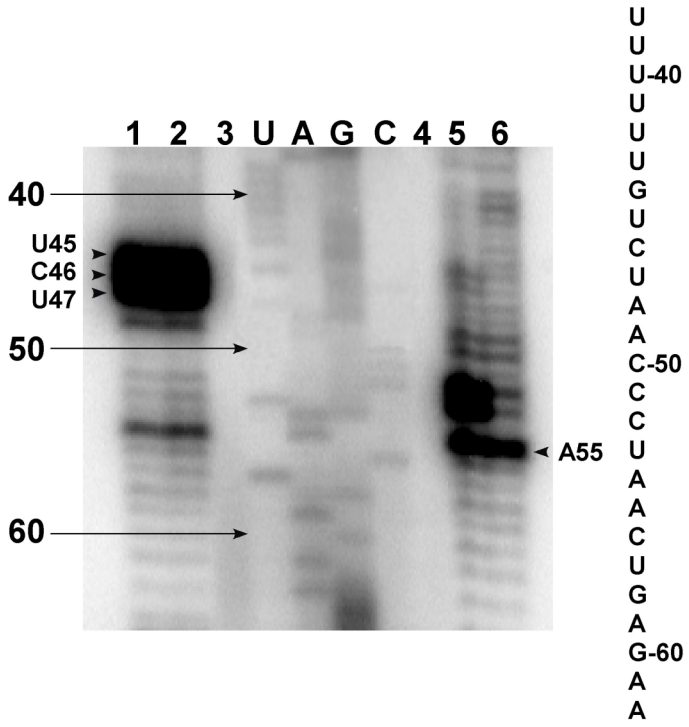

Figure 2.7. UV cross-linking reveals that the site of interaction within RNA33-147 is at the template domain. Sequencing gel of the cross-linking reaction between 4-thio-U hairpins and RNA33-147. Each lane contains a reverse transcriptase reaction as described in section 2.5. Lanes 1 and 2 are the s4U7 cross-linked products run in duplicate. Lane 3 is RNA33-147 reverse transcribed with only dNTPs. Lanes A, T, C, and G correspond to the sequencing ladder produced by dideoxy sequencing methods. Lane 4 is the reverse transcriptase reaction (only dNTPs) of UV irradiated RNA33-147. Lanes 5 and 6 are the s4U8 cross-linked products run in duplicate. Stops due to cross-linking at U45, C46, U47, and A55 are indicated.

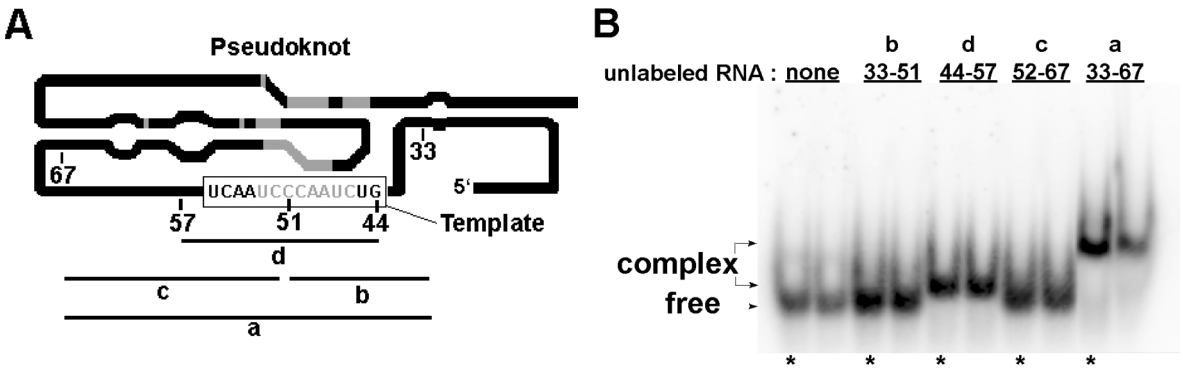

Figure 2.8. RNA-RNA interaction requires the entire hTR template domain. (A) Human telomerase RNA truncations analyzed for long-range RNA-RNA interaction with the P6.1 hairpin. Numbering corresponds to the hTR nucleotide sequence. The truncated RNA regions are (a) RNA33-67, (b) RNA33-51, (c) RNA52-67, and (d) RNA44-57. The bases in gray indicate 100% conserved nucleotides (Chen et al. 2000). (B) Gel shift assay with ^{32}P 5'-end labeled P6.1 hairpin and truncated RNA pieces from the 5' region of hTR. RNA33-51 and RNA52-67 contain sections of the template and show no complex formation. Only RNA33-67 and RNA44-57, which contain the entire template, produce complexes with the hairpin.

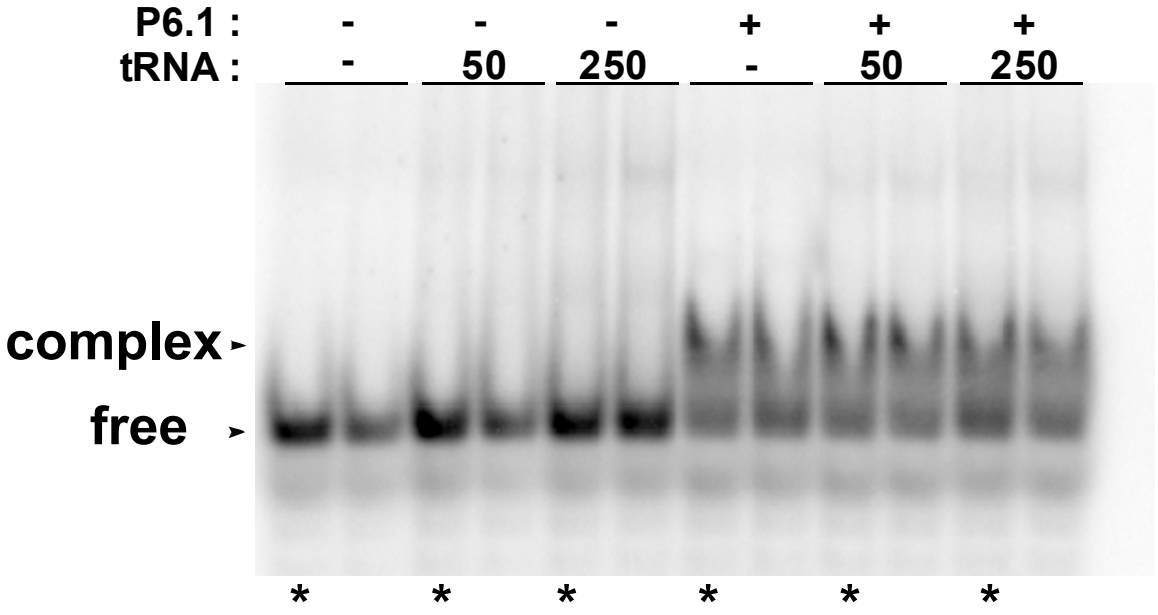

Figure 2.9. The 11-nucleotide templating and alignment domain (5'-CUAACCCUAAC-3') is minimally required for the long-range interaction with the P6.1 hairpin. The 11-nucleotide templating region is ^{32}P 5'-end labeled. The mobility-shift assay shows that competition with tRNA at concentrations of 50 μg/mL and 250 μg/mL does not alter the interaction. The numbers 50 and 250 indicate tRNA concentrations.

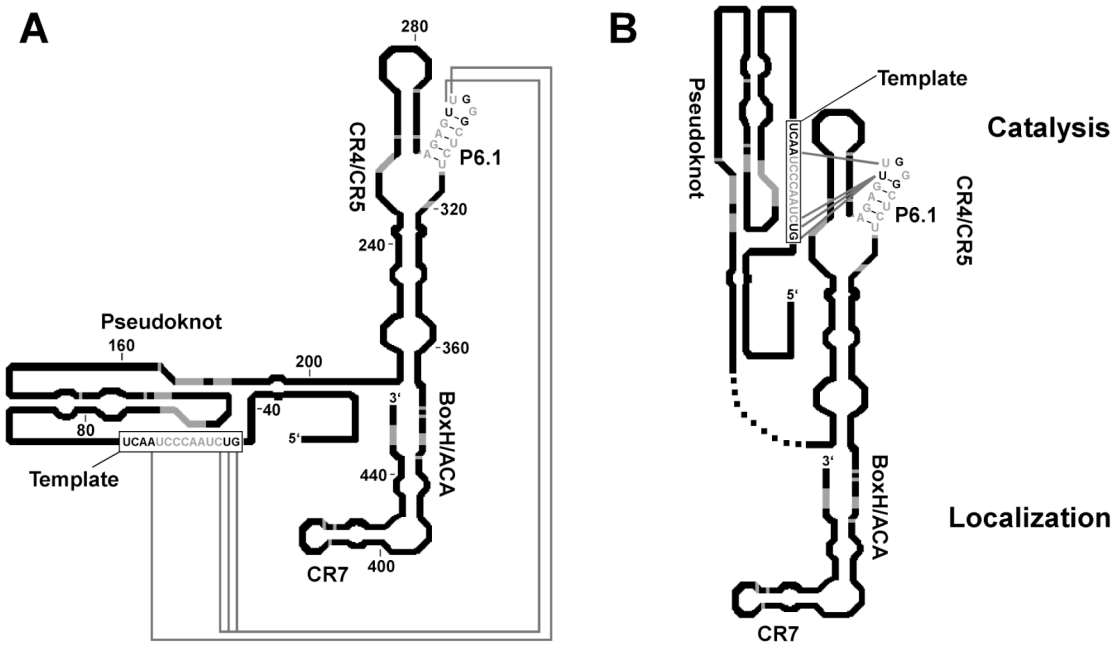

Figure 2.10. Models of human telomerase RNA. (A) Secondary structure of human telomerase RNA adapted from Chen et al. (2000) with the proposed long-range interactions revealed in this study indicated by gray connecting lines. (B) A new model for the secondary structure of hTR with interacting residues shown by gray connecting lines. The catalytic domains (pseudoknot, CR4/CR5 and template) and localization domains (box H/ACA and CR7) are indicated.

the presence of long-range RNA-RNA interactions possibly essential for overall architecture and function.

Studies by Mitchell and Collins (2000) show that deletion of residues 303-315 (P6.1) interferes with proper hTR and hTERT interaction and abrogates telomerase activity. Each of the 35 vertebrate RNAs has the capability of forming this short stem, indicating its importance in telomerase structure and function. Since deletion of this stem-loop interferes with the RNA-RNA interaction observed in this study, this higher order RNA-RNA interaction may have functional significance. Enzymatic mapping analysis shows that the loop bases of P6.1 (U307, G308 and G309) are accessible *in vitro* but inaccessible *in vivo* (Antal et al. 2002). Since these bases become protected in the presence of hTERT, it has been suggested that they associate with the protein. The recent NMR structure of P6.1 from Varani and co-workers shows that these bases are part of a well-defined structure that allows the exposed loop to participate in tertiary interactions with other portions of hTR or in RNA-protein interactions with hTERT (Leeper et al. 2003). Here, we show that P6.1 can participate in RNA-RNA interactions with the template of hTR. Based on our mutation analysis, the residues involved in the long-range RNA-RNA interactions are in the loop of P6.1.

Interaction between P6.1 and the template is mediated by the loop sequence and the formation of a stem. No complex forms when the stem is unable to base-pair. However, RNA-RNA interactions are maintained as long as the P6.1 stem forms, regardless of the stem sequence. Our P6.1 stem mutant analysis is consistent with studies on mouse telomerase RNA that showed that disruption of the P6.1 base-pairing in the stem abolishes telomerase activity (Chen et al. 2002).

Phylogenetic studies performed by Chen et al. (2000) show that positions 8 and 10 are 100% conserved. Therefore, these mutant hairpins are not expected to shift RNA33-147. Positions 7 and 9 are not 100% conserved; however, the shifts produced in the presence of the single base mutated hairpins are minimal compared to the shifts observed in the presence of the wild-type hairpin. Since the structure of the hairpin is critical for the RNA-RNA interaction, as evidenced by the stem mutant data, altering the P6.1 structure can lead to instability or abolishment of the interaction. The U7C mutation would alter the structure by replacing a U-G wobble pair with a G-C pair. U7 may be essential for the proper formation of the hairpin. G9 is positioned directly in the middle of the loop, suggesting that this exposed base would be a key participant in the interaction, and disruption of this critical base would lead to reduced binding affinity. Our results indicate that conservation of the loop residues (5'-UGG-3') is critical for the formation of the RNA-RNA interaction. These data are consistent with work accomplished by Greider and co-workers (Chen et al. 2002). Mutation of the loop sequence in the P6.1 stem-loop in mammalian telomerase RNA reduces telomerase activity, suggesting that mutation of this loop could disturb important RNA-RNA or RNA-protein interactions that contribute to the functional conformation at or near the catalytic center of telomerase.

Telomerase RNA structure has been characterized in ciliates (Romero and Blackburn 1991; Bhattacharyya and Blackburn 1994) as well as in humans (Chen et al. 2000; Antal et al. 2002). Studies on the *T. thermophila* telomerase RNA suggest that the template region of telomerase RNA is mostly single-stranded but possibly constrained to some conformation by folding of the rest of the RNA (Bhattacharyya and Blackburn 1994). Enzymatic mapping

studies from the Kiss group (Antal et al. 2002) show that U47 and C50 to C52 are not modified while C46 and U53 are weakly modified. Their results indicate that these bases participate in base-pairing interactions, protein-RNA interactions, or tertiary RNA structure. Additionally, bases adjacent to the template region are necessary for catalytic activity (Gavory et al. 2002; Miller and Collins 2002). When bases 54 and 56 are mutated, enzyme processivity is greatly reduced, indicating the importance of the conservation of these nucleotides (Chen and Greider 2003). We propose that these bases participate in critical long-range RNA-RNA interactions with residues in the CR4/CR5 domain.

Because both the P6.1 hairpin and the template region contain highly conserved bases, we believe that the interaction determined in our study has biological significance. In the current model of telomerase activity, telomeric repeats are added via a primer recognition step at the template, elongation, and translocation in preparation for the addition of the following repeat (Shippen-Lentz and Blackburn 1990). A regulatory mechanism involving the pseudoknot domain has recently been proposed (Comolli et al. 2002; Theimer et al. 2003). Both groups propose a molecular switch mechanism involving an equilibrium between the pseudoknotted and hairpin forms of the pseudoknot domain. For telomerase to be active, the pseudoknot domain must form.

We propose that other intramolecular RNA-RNA interactions, highlighted in figure 2.10, are involved in the higher order folding and consequently proper function of human telomerase RNA. Our results argue for the close proximity of the CR4/CR5 domain and the template. Since both are important for catalytic activity, the 5' portion of the RNA is likely closer to the CR4/CR5 domain than to the portions of the RNA important for nuclear

localization of the RNA (Lukowiak et al. 2001). As shown in figure 2.10B, the CR4/CR5, pseudoknot domain and template form the catalytic domain while the localization domain is composed of the box H/ACA and CR7 domains.

To investigate the link between the interaction observed in our study and its functional significance, we utilized mouse telomerase RNA constructs in gel mobility-shift assays. Based on functional data from Chen and Greider (2003), we expected mouse P6.1 to shift the human template since mouse CR4/CR5 and human pseudoknot, in the presence of hTERT or mTERT, can reconstitute activity. However, an interaction is not observed by mobility-shift assay (data not shown). Mouse P6.1 is also unable to shift the mouse template. Functionally, mouse and human telomerase differ in that human telomerase is processive, while mouse telomerase exhibits only a low level of processivity (Morin 1989; Prowse et al. 1993). If the P6.1/template interaction is involved in processivity, then mouse P6.1 would not be expected to interact similarly with the template. The telomerase protein may be able to compensate for the reduced binding affinity caused by the differences in sequence and structure between human P6.1 and mouse P6.1.

The entire template and alignment domain are necessary for the observed interaction. No gel shift is observed in the interaction assay between the P6.1 hairpin and RNAs containing only 5' or 3' portions of the template domain. This result, along with our cross-linking data, suggests that the hairpin may be interacting at multiple sites in the template domain. If the interaction is dynamic, the hairpin may be involved in the mechanism for translocation of the template during reverse transcription. In *Tetrahymena* telomerase, it has recently been shown that RNA sequences distant from the template are involved in mediating

nucleotide and repeat addition processivity (Lai et al. 2003). The conserved hairpin in the CR4/CR5 domain may play a similar role in human telomerase enzyme processivity. P6.1 may ready the template domain by either stabilizing the template or positioning it for proper reverse transcription by the protein. Further studies involving the protein will aid in the characterization of the functional significance of the RNA-RNA interaction revealed in this study.

2.5 Experimental

2.5.1 Synthesis of RNA

RNA was transcribed *in vitro* in transcription buffer (80 mM HEPES-KOH, pH 7.5; 2 mM spermidine; 40 mM DTT; 25 mM $MgCl_2$), 4 mM of each nucleotide triphosphate (CTP, ATP, UTP, GTP), RNAsecure (to prevent RNA degradation), 500 nM bottom strand (DNA template), 600 nM top strand (T7 primer), and T7 RNA polymerase at 37 ºC for 4 to 6 hours.

The following are the template sequences used for transcription of the indicated RNAs: **CR4/5-60** (5'-GGGCGGCTGACAGAGCCAACTTTGGTGGCTTTCGCCGACC GCGGCCTCCAGGCCCTATAGTGAGTCGTATTACGAATT-3'), **deltaP6.1** (5'-GGGCG GCTGACATTCGCGGTGGCTTTCGCCGACCGCGGCCTCCAGGCCCTATAGTGAG TCGTATTACGAATT-3'), **RNA33-67** (5'-CGCCCTTCTCAGTTAGGGTTAGACAAAAA ATGGCCTATAGTGAGTCGTATTACGAATT-3'), **RNA33-51** (5'-GGTTAGACAAAAA ATGGCCTATAGTGAGTCGTATTACGAATT-3'), **RNA44-57** (5'-AGTTAGGGTTAG ACTATAGTGAGTCGTATTACGAATT-3'), **RNA52-67** (5'-CGCCCTTCTCAGTTAGTA TAGTGAGTCGTATTACGAATT-3'), **RNAP6.1** (5'-GGAGAGCCCAACTCTCCGGTGG CTTTCGCCGACCGCGGCCTCCAGGCCCTATAGTGAGTCGTATTACGAATT-3').

The P6.1 hairpin mutants were transcribed like the wild-type hairpin with the single base or stem mutations as indicated in section 2.3.

RNA33-147 was synthesized by transcription off a template that was PCR-generated from a pUC19 plasmid containing the sequence encoding for RNA33-147. The PCR template (100 nM) was used for *in vitro* transcription with T7 RNA polymerase.

The following RNA oligonucleotides were ordered from the Caltech Oligonucleotide Synthesis Facility: **4-thio-U7** (5'-GGAGAG(s4U)UGGGCUCUCC-3'), **4-thio-U8** (5'-GGAG AGU(s4U)GGGCUCUCC-3'), **hTRtemplate (11-nucleotide)** (5'-CUAACCCUAAC-3'). All RNA synthesized by the synthesis facility required 2'-OTBDMS deprotection by use of triethylamine-3HF (Aldrich). After overnight deprotection in HF, the RNA samples were ethanol precipitated, dried, and resuspended in double distilled water (ddH_20).

All RNA products were gel purified by denaturing polyacrylamide gel electrophoresis (PAGE) in 1X TBE (90 mM Tris-borate, 2 mM EDTA). An electroelution apparatus was used to elute the RNA into 0.5X TBE. The RNA products were ethanol precipitated, dried to pellets, and resuspended in ddH_20. The concentrations were determined by UV spectroscopy and the biopolymer calculator developed by the Schepartz lab (Palmer 1998). Purity was assayed by analytical PAGE, mass spectrometry, or both.

2.5.2 ^{32}P 5'-end labeling

The terminal triphosphates of the transcribed RNA products were removed using calf intestinal phosphatase (Roche Diagnostics). The RNAs and DNA sequencing primers [**33-147seq** (5'-AAGGCGGCAGGCCGAGGC-3') and **tempseq** (5'-AGTCAGCGAGAAAAA CAGCG-3')] were kinased with T4 polynucleotide kinase (New England Biolabs) and

[γ^{32}P]ATP (NEN Life Science). The 5'-end labeled products were purified by NAP-25 columns (Amersham Pharmacia Biotech). Concentrations were assayed by scintillation counts based on an ATP standard, and adjusted to 20 nM.

2.5.3 Gel shift assay

The final concentrations of unlabeled RNA used in the gel shift assays were all 10 μM except in competition assays (concentrations indicated in the figure legends). The final concentration of the 5'-end labeled RNA was 5 nM. RNA binding buffers were adapted from Ferrandon et al. (1997). Each RNA was annealed by incubation in 1X binding buffer (high salt: 300 mM KCl; 5 mM $MgCl_2$; 50 mM sodium cacodylate, pH 7.5 or low salt: 40 mM KCl; 0.1 mM $MgCl_2$; 50 mM sodium cacodylate, pH 7.5) at 90 °C for ~1-2 minutes and then placed on ice for five minutes. The RNAs were then mixed and either placed on ice for 30 minutes or incubated at 37 °C for 30 minutes. Five μL of gel loading buffer (5X binding buffer, 50% glycerol) were added to each mixture before running on a 6% native polyacrylamide gel in 1X TBM (90 mM Tris-borate, 5 mM $MgCl_2$) maintained at 3-5 °C. The gels were run between two and three hours at 2-3 W, dried, and exposed to a PhosphorImager screen overnight. The gels were analyzed on a Storm860 and by ImageQuant.

2.5.4 4-thio-U cross-linking

The following 4-thiouridine cross-linking protocol was adapted from established protocols (Dubreuil et al. 1991). The 4-thio-U modified RNAs were 5'-end labeled with [γ^{32}P]ATP. The modified hairpin (10 μM) and RNA33-147 (10 μM) were separately incubated in 1X high salt binding buffer at 90 °C for two minutes and set on ice for five minutes. The RNAs were mixed together, set on ice, and irradiated with a handheld 365 nm UV light for 30

minutes. The RNAs were then ethanol precipitated, dried, and resuspended in ddH_20. The cross-linked sample was separated from uncross-linked material by running the reaction on a 12% denaturing PAGE in 1X TBE. The cross-linked product was excised from the gel, eluted into 0.5X TBE, ethanol precipitated, dried, and resuspended in ddH_20. Concentrations were determined by means of UV spectrometry (Palmer 1998).

2.5.5 Sequencing reactions

The cross-linked products and RNA33-147 were sequenced by Moloney Murine Leukemia Virus (MMLV) reverse transcription (Invitrogen) and the 5'-end labeled primers 33-147seq and tempseq. The sequencing reaction and UV cross-linking mapping protocols were adapted from established procedures (Lowe and Eddy 1999). For the RNA33-147 sequencing reaction, 2 μg RNA and 1.5 pmol labeled sequencing primer were incubated at 90 °C for two minutes in 1X annealing buffer (250 mM Tris-Cl, pH 8.0; 375 mM KCl; 50 mM dithiothreitol (DTT)) in a 10 μL annealing reaction. The annealed product was set on ice for two minutes.

For the primer extension reaction, four tubes (A, T, C, and G) were prepared. In each of the four tubes (A, T, C, or G) was placed: 2 μl of the annealed product (from above), 330 μM of each dNTP (A, T, C, and G), 1 mM of the appropriate ddNTP (A, T, C, or G) and MMLV RT buffer (250 mM Tris-Cl, pH 8.0; 375 mM KCl; 15 mM $MgCl_2$; 50 mM DTT; 1X Superase-In (Ambion, proprietary); 100U MMLV reverse transcriptase) to a total volume of 5 μL. The extension reactions were incubated at 42 °C for one hour, and then placed at 65 °C to heat inactivate the reverse transcriptase. Ten μL of sequencing dye (1X TBE; 80% formamide; bromophenol blue; xylene cyanol) was added to each tube and 5 μL of each reaction was loaded onto a 10% denaturing PAGE. The gel was run at 50W for 2-2.5 hours in

1X TBE. The sequencing gel was fixed with destain solution (40% methanol; 10% acetic acid; 50% water) for 30 minutes prior to drying. The dried gels were exposed to screens overnight and imaged by the PhosphorImager.

The cross-linked products were sequenced as above with the following changes. Only one tube was necessary for the primer extension reaction. This tube contained no ddNTPs. The stops occurred as a result of the cross-links. The sequencing reaction and the mapping reaction of the cross-linked products were run adjacently on a sequencing gel as described above. The cross-links were identified by stops in the mapping reaction ladder and the base of interaction read from the sequencing ladder.

Bibliography

Antal, M., E. Boros, F. Solymosy, and T. Kiss. 2002. Analysis of the structure of human telomerase RNA *in vivo*. *Nuc. Acids Res.* **30**: 912-920.

Autexier, C. and C. W. Greider. 1994. Functional reconstitution of wild-type and mutant *Tetrahymena* telomerase. *Genes Dev.* **8**: 563-575.

Bachand, F. and C. Autexier. 2001. Functional regions of human telomerase reverse transcriptase and human telomerase RNA required for telomerase activity and RNA-protein interactions. *Mol. Cell Biol.* **21**: 1888-1897.

Bhattacharyya, A. and E. H. Blackburn. 1994. Architecture of telomerase RNA. *EMBO J.* **13**: 5721-5731.

Beattie, T. L., W. Zhou, M. O. Robinson, and L. Harrington. 2000. Polymerization defects within human telomerase are distinct from telomerase RNA and TEP1 binding. *Mol. Biol. Cell* **11**: 3329-3340.

Blackburn, E. H. 1991. Structure and function of telomeres. *Nature,* **350**: 569-573.

Blackburn, E. H. 2000. The end of the (DNA) line. *Nat. Struct. Biol.* **7**: 847-850.

Cech, T. R. 2000. Life at the end of chromosomes: telomeres and telomerase. *Angew. Chem. Int. Ed.* **39**: 34-43.

Chen, J. L., M. A. Blasco, and C. W. Greider. 2000. Secondary structure of vertebrate telomerase RNA. *Cell* **100**: 503-514.

Chen, J. L. and C. W. Greider. 2003. Determinants in mammalian telomerase RNA that mediate enzyme processivity and cross-species incompatibility. *EMBO J.* **22**: 304-314.

Chen, J. L., K. K. Opperman, and C. W. Greider. 2002. A critical stem-loop structure in the CR4-CR5 domain of mammalian telomerase RNA. *Nuc. Acids Res.* **30**: 592-597.

Comolli, L. R., I. Smirnov, L. Xu, E. H. Blackburn, and T. L. James. 2002. A molecular switch underlies a human telomerase disease. *Proc. Natl. Acad. Sci. USA* **99**: 16998-17003.

Corey, D. R. 2002. Telomerase inhibition, oligonucleotides, and clinical trials. *Oncogene* **21**: 631-637.

Dubreuil, Y. L., A. Expert-Benzancon, and A. Favre. 1991. Conformation and structural fluctuations of a 218 nucleotides long rRNA fragment: 4-thiouridine as an intrinsic photolabeling probe. *Nuc. Acids Res.* **19**: 3653-3660.

Feng, J., W. D. Funk, S. Wang, S. L. Weinrich, A. A. Avilion, C. Chiu, R. R. Adams, E. Chang, R. C. Allsopp, J. Yu, S. Le, M. D. West, C. B. Harley, W. H. Andrews, C. W. Greider, and B. Villeponteau. 1995. The RNA component of human telomerase. *Science* **269**: 1236-1241.

Ferrandon**,** D., I. Koch, E. Westhof, and C. Nüsslein-Volhard. 1997. RNA-RNA interaction is required for the formation of specific *bicoid* mRNA 3' UTR-STAUFEN ribonucleoprotein particles. *EMBO J.* **16**: 1751-1758.

Gavory, G., M. Farrow, and S. Balasubramanian. 2002. Minimum length requirement of the alignment domain of human telomerase RNA to sustain catalytic activity *in vivo*. *Nuc. Acids Res.* **30**: 4470-4480.

Greider, C. W. and E. H. Blackburn. 1985. Identification of a specific telomere terminal transferase activity in *Tetrahymena* extracts. *Cell* **43**: 405-413.

Greider, C. W. and E. H. Blackburn. 1989. A telomeric sequence in the RNA of *Tetrahymena* telomerase required for telomerase repeat synthesis. *Nature* **337**: 331-337.

Hahn, W. C., C. M. Counter, A. S. Lundberg, R. L. Beijersbergen, M. W. Brooks, and R. A. Weinberg. 1999. Creation of human tumour cells with defined genetic elements. *Nature* **400**: 464-468.

Kim, N. W., M. A. Piatyszek, K. R. Prowse, C. B. Harley, M. D. West, P. L. Ho, G. M. Coviello, W. E. Wright, S. L. Weinrich, and J. W. Shay. 1994. Specific association of human telomerase activity with immortal cells and cancer. *Science* **266**: 2011-2015.

Lai, C. K., M. C. Miller, and K. Collins. 2003. Roles for RNA in telomerase nucleotide and repeat addition processivity. *Mol. Cell* **11**: 1673-1683.

Leeper, T., N. Leulliot, and G. Varani. 2003. The solution structure of an essential stem-loop of human telomerase RNA. *Nuc. Acids Res.* **31**: 2614-2621.

Lingner, J., T. R. Hughes, A. Shevchenko, M. Mann, V. Lundblad, and T. R. Cech. 1997. Reverse transcriptase motifs in the catalytic subunit of telomerase. *Science* **276**: 561-567.

Lowe, T. M. and S. R. Eddy. 1999. A computational screen for methylation guide snoRNAs in yeast. *Science* **283**: 1168-1171.

Lukowiak, A. A., A. Narayanan, Z. Li, R. M. Terns, and M. P. Terns. 2001. The snoRNA domain of vertebrate telomerase RNA functions to localize the RNA within the nucleus. *RNA* **7**: 1833-1844.

Martín-Rivera, L. and M. Blasco. 2001. Identification of functional domains and dominant negative mutations in vertebrate telomerase RNA using an *in vivo* reconstitution system. *J. Biol. Chem.* **276**: 5856-5865.

Miller, M. C. and K. Collins. 2002. Telomerase recognizes its template by using an adjacent RNA motif. *Proc. Natl. Acad. Sci.* **99**: 6585-6590.

Mitchell, J. R., J. Cheng, and K. Collins. 1999. A box H/ACA small nucleolar RNA-like domain at the human telomerase RNA 3' end. *Mol. Cell Biol.* **19**: 567-576.

Mitchell, J. R. and K. Collins. 2000. Human telomerase activation requires two independent interactions between telomerase RNA and telomerase reverse transcriptase. *Molecular Cell* **6**: 361-371.

Morin, G.B. 1989. The human telomerase terminal transferase enzyme is a ribonucleoprotein that synthesizes TTAGGG repeats. *Cell* **59**: 521-529.

Nakamura, T. M., G. B. Morin, K. B. Chapman, S. L. Weinrich, W. H. Andrews, J. Lingner, C. B. Harley, and T. R. Cech. 1997. Telomerase catalytic subunit homologs from fission yeast and human. *Science* **277**: 955-959.

Palmer, C. R. 1998. *Biopolymer Calculator.* Available at http://paris.chem.yale.edu/extinct.html, accessed September 17, 2003.

Prowse, K. R., A. A. Avilion, and C. W. Greider. 1993. Identification of a nonprocessive telomerase activity from mouse cells. *Proc. Natl. Acad. Sci. USA* **90**: 1493-1497.

Rezler, E. M., D. J. Bearss, and L. H. Hurley. 2002. Telomeres and telomerase as drug targets. *Curr. Opin. Pharm.* **2**: 415-423.

Romero, D. P. and E. H. Blackburn. 1991. A conserved secondary structure for telomerase RNA. *Cell* **67**: 343-353.

Shippen-Lentz, D. and E. H. Blackburn. 1990. Functional evidence for an RNA template in telomerase. *Science* **247**: 546-552.

Theimer, C. A., L. D. Finger, L. Trantirek, and J. Feigon. 2003. Mutations linked to dyskeratosis congenita cause changes in the structural equilibrium in telomerase RNA. *Proc. Natl. Acad. Sci. USA* **100**: 449-454.

Tesmer, V. M., L. P. Ford, S. E. Holt, B. C. Frank, X. Yi, D. L. Aisner, M. Ouellete, J. W. Shay, and W. E. Wright. 1999. Two inactive fragments of the integral RNA cooperate to assemble active telomerase with the human protein catalytic subunit (hTERT) *in vitro*. *Mol. Cell Biol.* **19**: 6207-6216.

APPENDIX A:

UNDERSTANDING THE ENRICHMENT PROCESS OF MRNA DISPLAY

The experiments for this section were performed in large part by Cheryl Chow.

Appendix A

UNDERSTANDING THE ENRICHMENT PROCESS OF MRNA DISPLAY

A.1 Introduction

Currently, the standard method for determining how a selection is progressing is via the ^{35}S binding assay described in section 3.5.3. This technique provides a quick, easy metric for success, and can be done concurrent with a selection. At the end of the selection, however, we do not know when the "winner" sequence came to be a significant part of the pool or if all rounds of selection were necessary to produce the winner. In order to address these questions, we turned to quantitative PCR (qPCR). qPCR allows for the quantification of starting amounts of DNA, cDNA, and RNA templates in a sample. We chose to utilize qPCR for two purposes: (1) to determine the actual number of any one sequence present in each round and (2) to develop a more sensitive approach to establish library diversity.

A.2 Utilizing Quantitative PCR for Understanding the Enrichment Process of mRNA Display

To address the first purpose, we used qPCR to determine the number of 18-8 sequences present in the rounds of the P6.1 selection presented in chapter 3. These numbers allow us to quantitatively measure the amount of enrichment from round to round. We tested rounds 0, 1, 3, 6, 10, 11, 12, 13, 14, 15, 16, and 18. These rounds were chosen based on the ^{35}S binding data obtained from the P6.1 selection (figure 3.3A). We PCR amplified the DNA

from each round (as described in section 3.5.2), gel purified them using the QiaQuick PCR Purification Kit (Qiagen), and tested them via qPCR. The DNA concentrations were determined using the NanoDrop (NanoDrop Technologies). Each reaction contained 12.5 μL Bio-Rad iQ SYBR Green Supermix, 0.5 ng DNA, 200 nM primers (18-8L: 5'-ATTTACAATTACAATGACGACGAG-3' and 18-8R: 5'-AGGAGGCGGACCCTGTAGTA-3') in a total volume of 25 μL.

Preliminary results from the qPCR experiment are shown in table A.1 and figure A.1. The data show very little, if any, enrichment between rounds 0 through 6. From round 10 through 15, an increase in the 18-8 sequence is observed. An apparent drop in the fraction of 18-8 sequences is seen in rounds 16 and 18, but these may be artifacts of the experiment and further testing is required to determine if this drop is consistently seen.

These data tell us about the population of 18-8 in the pool of sequences as a function of each round. The most significant increase in 18-8 sequence occurred from round 11 to 12, but the 18-8 sequence did not reach 50% abundance until round 13. Between rounds 13 and 15, 18-8 comes to completely dominate the pool. Therefore, rounds 16 through 18 likely did not produce any further enrichment. This analysis suggests that the selection may have been too stringent (e.g., too many rounds or too much competitor tRNA), resulting in only one selected sequence. Future experiments will include sequencing clones from rounds 13 and 14 to determine if other families of sequences that bind to the P6.1 hairpin exist.

Both the qPCR data and the ^{35}S binding assay provide important information about a selection since qPCR allows for the quantification of any one sequence in each round, while the ^{35}S binding data provides a functional metric for the progress of a selection. According to

Table A.1. Copy number and percentage of the 18-8 sequence present in each round of selection.

Round	Raw SQ	ADJ SQ	18-8%
round 0	8.63E+03	2.11E+00	0.00%
round 1	4.32E+03	5.27E-01	0.00%
round 3	7.62E+02	9.31E-02	0.00%
round 6	4.83E+04	5.90E+00	0.00%
round 10	1.88E+07	2.29E+03	0.62%
round 11	8.83E+07	1.08E+04	2.94%
round 12	6.40E+08	1.56E+05	21.24%
round 13	1.48E+09	3.61E+05	49.16%
round 14	2.11E+09	5.14E+05	69.92%
round 15	2.99E+09	7.30E+05	99.32%
round 16	2.70E+09	6.58E+05	89.52%
round 18	2.29E+09	5.60E+05	76.23%
18-8	3.76E+09	2.29E+05	124.90%

Raw SQ=Raw data (copy number) obtained from quantitative PCR; ADJ SQ=Copy number corrected for the first universal PCR amplification, representing the actual number of the 18-8 sequence in each round of selection; 18-8%=Percent of total sequences that are the 18-8 sequence. The 18-8% values are based on the PCR efficiency, which can be greater than 100% due to nonspecific PCR products amplified during the experiment.

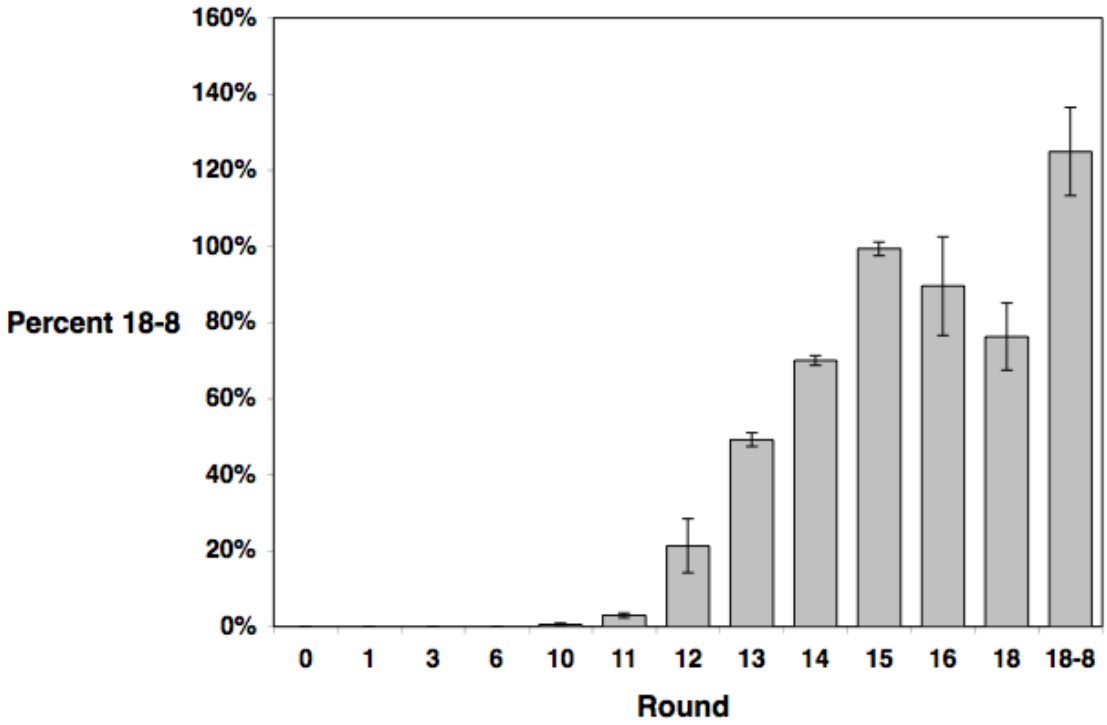

Figure A.1. Percentage of 18-8 sequence in each round of selection. 18-8 represents a control experiment where only the 18-8 sequence is PCR amplified.

the qPCR data, the 18-8 sequence reached 50% abundance by round 13, but the ^{35}S binding data did not indicate substantial binding until round 15. The qPCR data indicates that the selection may have converged by round 15, but we continued the selection since the ^{35}S binding data indicated the library was still changing substantially between rounds 15 and 17. The qPCR data suggests that when the ^{35}S binding assay begins to show an increase in binding, we should sequence the pool to avoid potential over-selection. The discrepancy in the ^{35}S binding data and the qPCR analysis may be due to experimental bias. As shown in figure A.1, the PCR efficiency can be greater than 100%; this can result from nonspecific PCR products (e.g., primer dimer), PCR inhibitors in the reaction, or suboptimal primer and template concentrations.

A disadvantage of the qPCR method is that we cannot monitor the changing population during a selection since this method requires knowledge of the winning sequence. It does, however, present an interesting historical look into the progression of a selection, and will allow us to return to archived pools for further sequencing and characterization.

A.3 Using Dissociation Curves to Establish Library Diversity

At the conclusion of a qPCR experiment, it is possible to produce dissociation curves from a standard DNA melt experiment. The double-stranded qPCR products are slowly heated to monitor the dissociation of the two strands. Recent studies have utilized these qPCR dissociation curves to determine sequence diversity in genes (Schwalbach and Fuhrman 2005), and detect sequence variants containing as few as three base pair mutations (Papin et al. 2004). We hoped to utilize dissociation curves to reveal library diversity from round to round in the selection presented in chapter 3.

The DNAs from selected rounds were PCR amplified using the universal primers (47T7 5' primer and 3X27 3' primer) described in chapter 3 using the MyIQ real-time PCR machine (Bio-Rad). The PCR products were then brought to 50 °C, and slowly heated in half-degree steps to 95 °C. The PCR is monitored via a fluorescent dye, SYBR green (Bio-Rad). As PCR products are made, the fluorescent dye binds the double-stranded DNA, resulting in an increase in fluorescence. As the PCR products are denatured during the melt experiment, the SYBR green fluorescent dye is released from the DNA, and the fluorescence decreases. The dissociation curve in figure A.2 shows the derivative (−d(RFU)/dt) of the fluorescence value versus temperature. The breadth of the peaks can be used as an indication of changing library diversity since broader peaks suggest a more diverse population while narrower peaks imply fewer unique sequences. The data in figure A.2 show that the breath of the peaks changes between the early and late rounds, where the average difference between the beginning of the melt and the end of the melt for early rounds is ~20 °C and for late rounds it is only ~10 °C. The melting temperature also changes, though this change may not be a feature of all selections; in some selections, the melting temperature may increase, decrease or remain constant. For the P6.1 selection, the melting temperature for early rounds (0, 3, and 6) is ~74 °C while later rounds (10, 12, 14, and 16) have significantly higher melting temperatures. Rounds 10 through 16 see an increasing melt temperature with the 18-8 sequence melting at ~90 °C. In the P6.1 selection, the change in melting temperature accompanies the change in library diversity.

Narrowing of the dissociation curve is indicative of the changing library diversity in a successful selection. As the dissociation curve narrows, the library will contain fewer unique

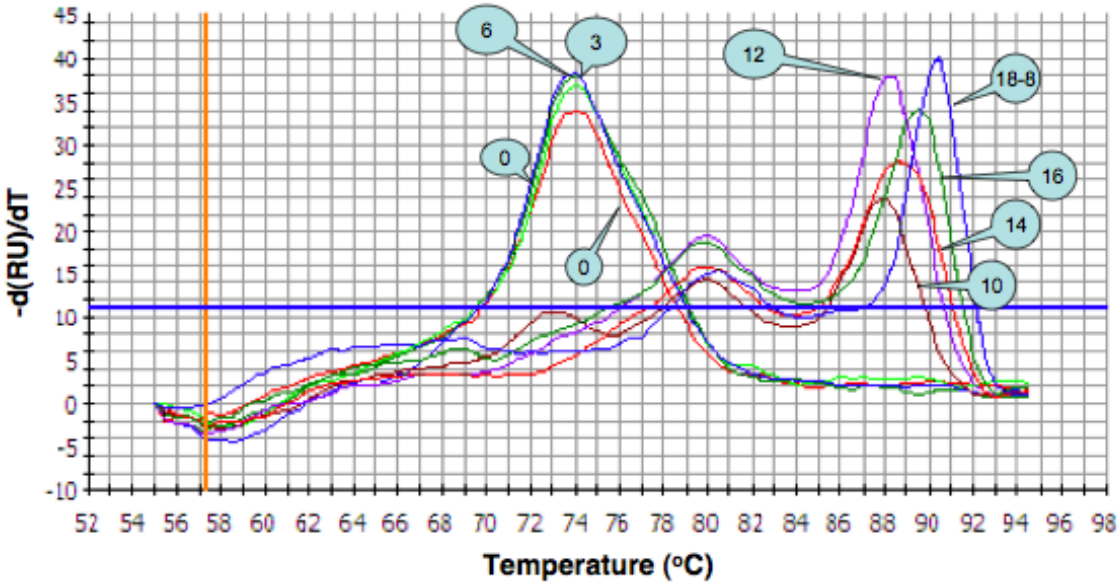

Figure A.2. Dissociation curves for several rounds of the selection. Numbers in circles indicate the DNA round from which the product was amplified. Early rounds (0, 3, and 6) have broader dissociation curves compared to later rounds (10, 12, 14, and 16).

sequences. An accompanying change (increase or decrease) in melting temperature may also serve as a secondary gauge of changing library diversity. These observation may prove to be general indicators of the progress of a selection, and signal that the selection has converged when the dissociation curve stops changing. This method for monitoring a selection is useful in that it requires no radioactivity, and can be done concurrently with the selection since knowledge of any one sequence is unnecessary for the qPCR amplification and analysis.

Bibliography

Papin, J. F., W. Vahrson, D. P. and Dittmer. 2004. SYBR green-based real-time quantitative PCR assay for detection of West Nile virus circumvents false-negative results due to strain variability. *J. Clin. Microbiol.* **42**: 1511-1518.

Schwalbach, M. S. and J. A. Fuhrman. 2005. Wide-ranging abundances of aerobic anoxygenic phototrophic bacteria in the world ocean revealed by epifluorescence microscopy and quantitative PCR. *Limnol. Oceanogr.* **50**: 620-628.

APPENDIX B:

REDESIGNING HTR TARGETS FOR MRNA DISPLAY

Appendix B

REDESIGNING HTR TARGETS FOR MRNA DISPLAY

B.1 Introduction

We are interested in targeting human telomerase RNA via mRNA display. The peptides we isolate will bind specifically and with high affinity to catalytically critical regions of hTR, and will represent promising leads for antitumor-specific therapies. The selection described in chapter 3 resulted in a peptide that binds the dimeric form of the catalytically important P6.1 hairpin. In an effort to make a better-behaved target for *in vitro* selection via mRNA display, we redesigned the P6.1 target and utilized the X27 library in a selection against the new target.

B.2 Designing a New hTR P6.1 Target

In order to make a target that had a lower propensity to dimerize, we extended the stem of the P6.1 target to produce two targets, the 26P6.1 and the 28P6.1 targets (figure B.1). Using the DNA templates: **26P6.1** (5'-TTTTAGGAGAGCCCAACTCTCCTACCTATAG TGAGTCGTATTACGAATT-3') and **28P6.1** (5'-TTTGGTAGGAGAGCCCAACTCTC CTACCTATAGTGAGTCGTATTACGAATT-3'), the RNAs were transcribed in 1 mL reactions and purified as described in section 2.5.1. The RNAs were then ^{32}P-end labeled (section 2.5.2). The two RNAs were utilized in a time-course experiment to determine the amount of dimer formation over time. Each reaction contained 50 μM unlabeled RNA (with

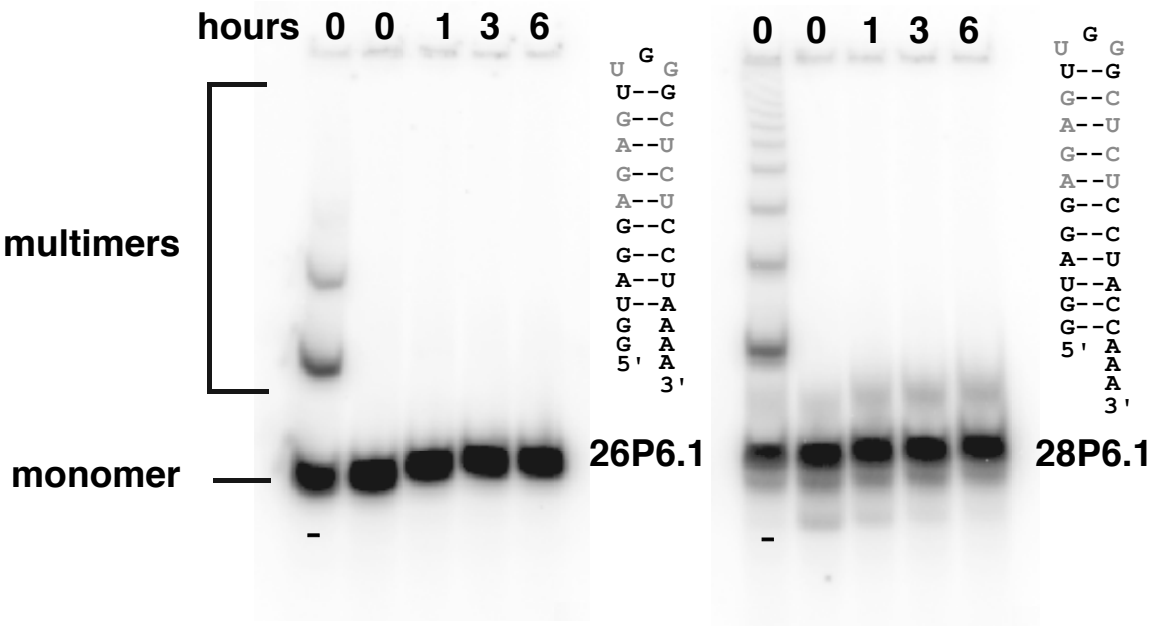

Figure B.1. Time course for dimer formation of the new P6.1 targets. Gray bases indicate 100% conservation across all vertebrate telomerase RNAs (Chen et al. 2000). The "-" indicates that the sample was not annealed prior to loading to the native gel.

~100,000 counts of ^{32}P-labeled RNA added to the sample for PhosphorImaging), 0.5X TBE, and 10% glycerol. The RNAs were annealed at 90 °C for 90 seconds, followed by two minutes on ice, and then left at room temperature for 0, 1, 3, or 6 hours. Unannealed RNA samples were used as controls to determine the amount of dimer present without the annealing step. The reactions were run on a 10% native gel in 0.5X TBE at 5 °C for ~1.5 hours at 3W. The gel was then dried and exposed overnight to a PhosphorImager screen. The screen was scanned in a Storm860 and visualized using ImageQuant software. As seen in figure B.1, both 26P6.1 and 28P6.1 exist as monomers and multimers when no annealing is performed. However, when the RNAs are annealed, the targets are mostly monomeric. 26P6.1 is better behaved, since no multimeric species are observed by gel after 6 hours at room temperature while 28P6.1 exhibits formation of a dimeric species over time. Therefore, 26P6.1 was chosen as a new target for selection.

B.3 Modified Protocol for Selection against 26P6.1

The selection protocol from section 3.5 was modified to (1) prevent the isolation of a dimer-binding peptide and (2) make the selection converge in fewer rounds. To determine if the multimeric forms of 26P6.1, and not the monomeric target bound the 18-8peptide, a mobility-shift experiment was performed (figure B.2). Each reaction contained 5 nM ^{32}P-labeled 26P6.1 RNA in selection buffer. Lanes 2 and 4 also contain 100 nM 18-8 peptide. In lanes 1 and 2 the 26P6.1 RNA has not been annealed, while the RNA has been annealed in lanes 3 and 4. As seen in figure B.2, the 18-8 peptide binds to the multimeric forms of the 26P6.1 target, and not to the monomeric form (lane 2). We therefore added 100 nM 18-8

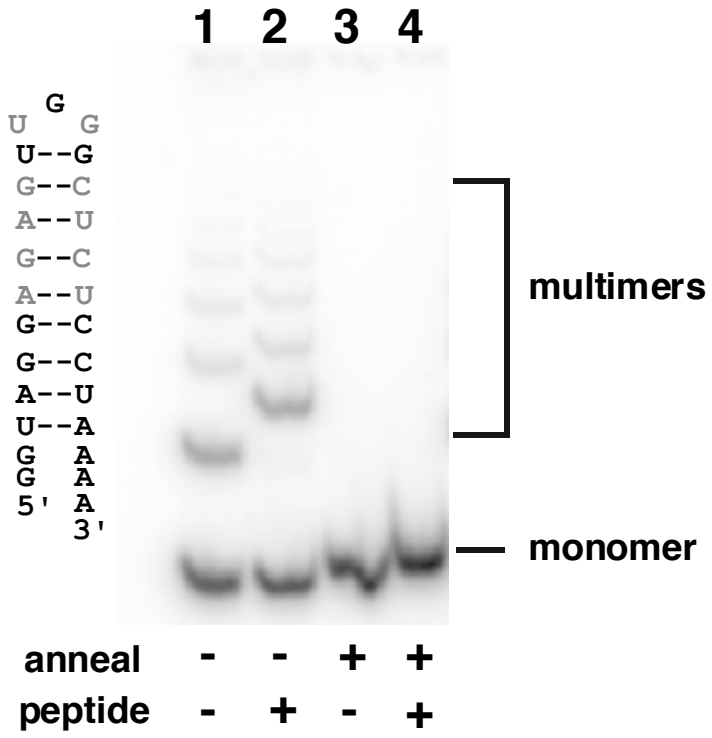

Figure B.2. Analysis of the new 26P6.1 target. The peptide used is the 18-8 peptide described in chapter 3. The "-" indicates no peptide (lanes 1 and 3) or no annealing (lanes 1 and 2) while the "+" indicates addition of 100 nM peptide (lanes 2 and 4) or annealing (lanes 3 and 4). The 18-8 peptide binds the multimers and not the monomeric form of 26P6.1.

peptide as a specific competitor to the selective step and the wash steps so that any dimer present on the beads would be bound by 18-8 and not by mRNA-peptide fusions.

In order to make the selection converge in fewer rounds, we added an extra purification step utilizing Thiopropyl (TP) Sepharose 6B (Amersham). The structure of the Thiopropyl Sepharose 6B and the reaction mechanism involved in the purification are shown in figure B.3. Since the TP sepharose retains molecules containing free thiols, peptides containing a cysteine will be separated from non-cysteine containing molecules. Therefore, in order to utilize the TP sepharose purification, a cysteine had to be added to the constant region of each peptide. Utilizing a revised 3' primer for amplification of the X27 library: 3X27CA (5'-GGCGCAAATAGCGGATGCACGCAGACC-3') and a revised splint for the splint ligation step: X27CAsplint (5'-TTTTTTTTTTTTNGGCGCAAATAGCGGATG-3'), we successfully incorporated a cysteine into each peptide. The new library was called X27CA.

The TP sepharose beads were prepared by adding 1 mL 0.1% Triton-X to 50 mg dry TP sepharose. The beads were washed with 1 mL 1X TE buffer pH 8.0 five times, then made into a 50:50 w/v slurry in 1X TE. After the dT purification step, 50 μL 50:50 w/v TP sepharose beads and 500 μL of dT purified mRNA-peptide fusions were incubated in 50 mM NaOAc buffer, pH 4.5 for two hours at 4 °C. The beads were transferred to a 0.45 μm Spin-X column and washed with 700 μL of 50 mM NaOAc buffer, pH 4.5 at 4 °C three times. The suspension was spun down between each wash, and the flow-through removed. The beads were then resuspended in two 250 μL fractions of 50 mM DTT, 1X TBE and incubated at 4 °C for one hour. The beads were then spun down in a clean 0.45 μm Spin-X column and the flow-through, which contained the purified fusions, was ethanol precipitated. The reactions

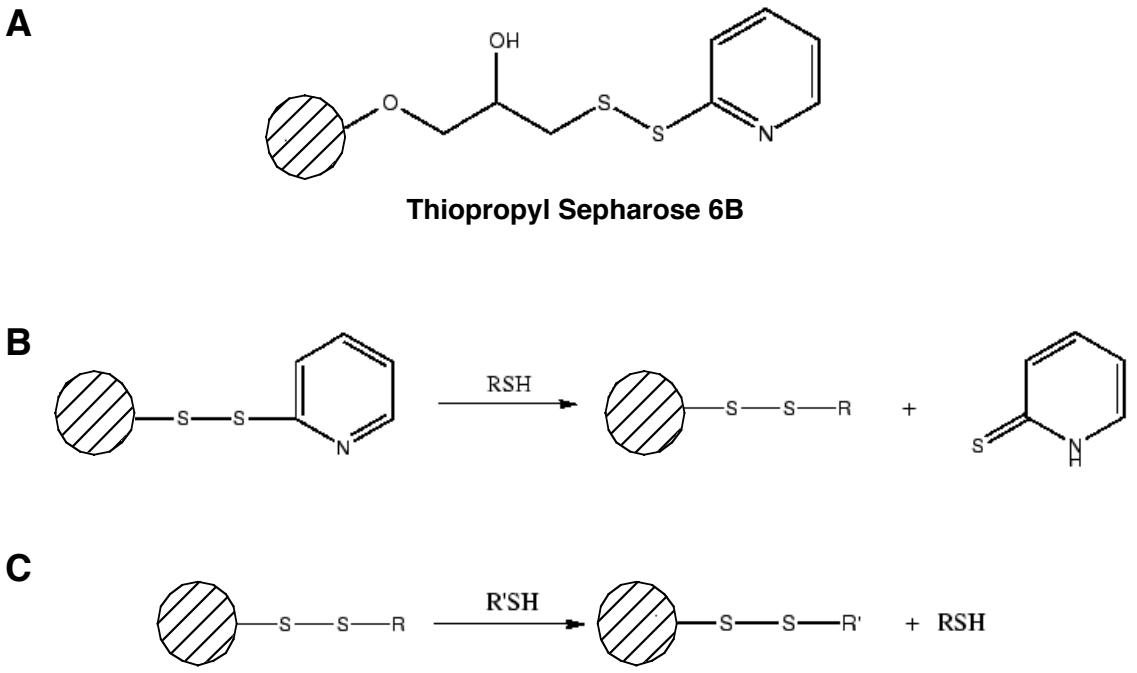

Figure B.3. Thiopropyl (TP) sepharose purification scheme. A) Structure of Thiopropyl Sepharose 6B. The circle with diagonal lines represents the matrix. B) Reaction of activated Thiopropyl Sepharose 6B with thiols (RSH). C) Release of bound thiols (RSH) upon reaction with a second thiol (R'SH).

were then spun down to pellets and resuspended in 15 μL ddH_20 for the reverse transcription step.

Figure B.4 shows where the TP sepharose purification step was incorporated. After translation, fusion formation, and dT purification, mRNA-peptide fusions as well as mRNA with no peptide attached remain. This occurs because the efficiency of fusion formation is typically only ~10% to 20% for this system (data not shown). A TP sepharose purification step would eliminate most of the unfused mRNA (mRNA with no peptide attached) because the TP sepharose retains the cysteine-containing peptides; this results in a higher overall percentage of mRNA-peptide fusions going into the selective and amplification steps. This will yield an increase in enrichment from round to round because less nonspecific material would be carried through each round. A control experiment was performed to determine how much enrichment the TP sepharose purification would add. Figure B.5 shows the PCR products after a round that did (+TP) and did not (-TP) undergo TP sepharose purification. Untranslated (U) material represents nonspecific, nonpeptidic material that is carried through the selection. Translated (T) material has mRNA-peptide fusions as well as some unfused mRNA that has not been purified away. The data indicate that the TP sepharose purification increases enrichment by ~10-fold, which is what would be expected assuming fusion formation efficiency is ~10%.

B.4 Selection against 26P6.1

Using 18-8 peptide as a competitor, as well as adding the TP sepharose purification step, a selection was performed against the 26P6.1 target. After 8 rounds of selection, the ^{35}S binding assay data indicated the library had converged (figure B.6). Instead of the 18 rounds

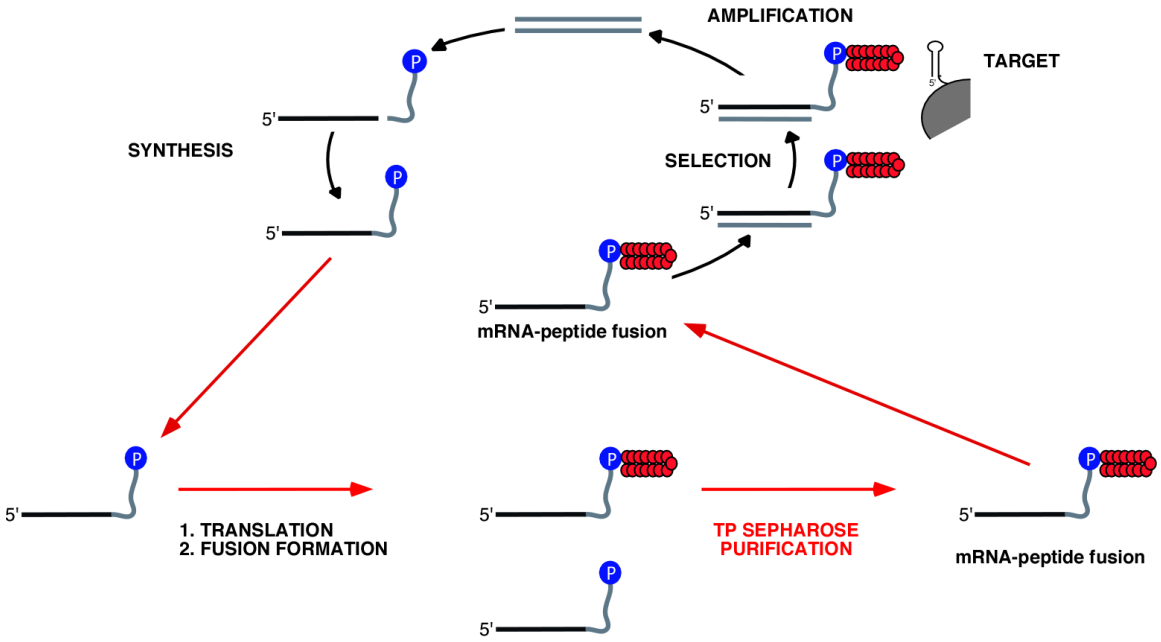

Figure B.4. A modified selection cycle incorporating a TP sepharose purification step. The TP purification step should remove most of the unfused mRNA (the mRNA with no peptide attached).

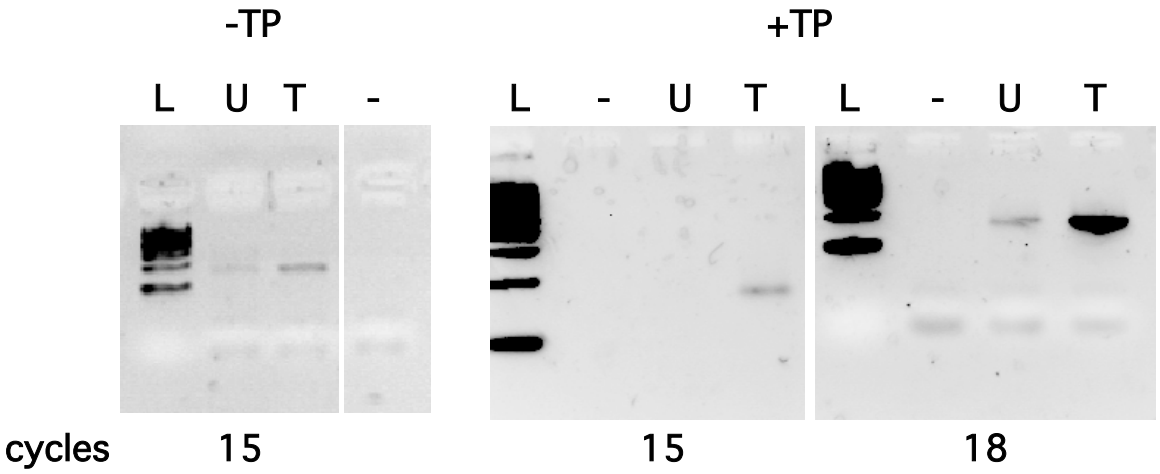

Figure B.5. Agarose gels of PCR products from a TP sepharose control experiment. –TP= no TP sepharose purification, +TP=TP sepharose purified, L=ladder, U=untranslated mRNA, T=translated mRNA, -=no template control. The number below each gel indicates the number of PCR cycles used to amplify the DNA product. This gel shows that the TP sepharose step increases enrichment by 10-fold.

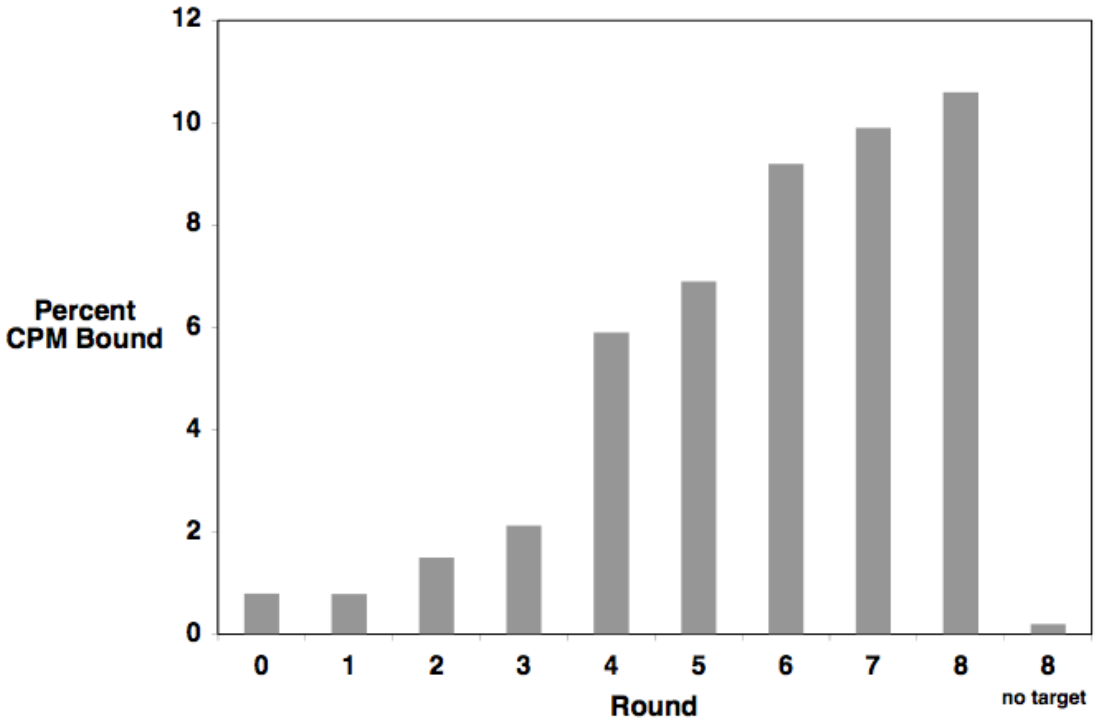

Figure B.6. Binding assay data for rounds of selection against 26P6.1. Percent CPM (counts per minute) bound indicates the percent of ^{35}S counts retained on the solid support during the binding assay. Binding increases over eight rounds of selection. A round 8 no target control is shown to indicate the amount of binding to the matrix only; this value should be low if the observed binding is due to specific interaction with the 26P6.1 target.

that were necessary for the X27 library to converge, only 8 rounds were required for the X27CA library, indicating that the TP sepharose purification step did increase the enrichment of each selective step. While ^{35}S binding data using mRNA-peptide fusions indicates that the round 8 pool binds to the 26P6.1 target, it does not bind to the old P6.1 target (data not shown). The selected peptides may bind to the extended stem or to the unpaired ends of the 26P6.1 target, shown in the red oval in figure B.7.

The sequences obtained from the X27CA library are shown in figure B.8. We obtained several unique sequences that are lysine and arginine rich. Though there is no apparent consensus sequence, we note that the occurrence of lysine and arginine residues in the 28 amino acid random region is highest in the N-terminal region and decreases in an N to C direction. Individual peptide sequences (1, 2, 3, 4, 6, 8, and 10) were assayed, but did not bind to the 26P6.1 target (data not shown). The DNA linker region, the mRNA, or both may be necessary for binding.

Selection using the X27CA library against 26P6.1 proves that the P6.1 RNA sequence is difficult to target. In chapter 3, we isolated a peptide that binds the dimeric form of the P6.1 RNA even though our target was designed to be greater than 90% monomeric. The selection presented in this section shows that the peptides evaded our sequence of interest and bound to the extended stem and unpaired region of the new 26P6.1 target. Other avenues of design that force the hairpin into a stable monomer, including psoralen cross-linking or ligation, may be necessary to make a successful P6.1 target. Alternatively, choosing other important regions of hTR, like the pseudoknot, box H/ACA, or CR7 domains as targets for selection may yield molecules that will bind biologically relevant structural elements in hTR.

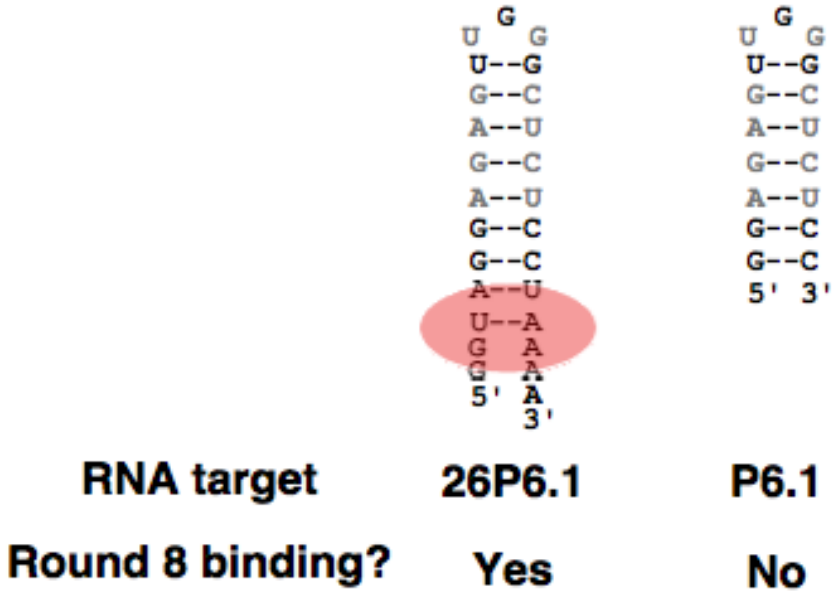

Figure B.7. Binding of round 8 mRNA-peptide fusions. Round 8 molecules bound to the 26P6.1, but not the P6.1 target, indicating the binding event likely occurs in the stem region highlighted by the red oval.

```
   1           11          21        constant region   (number)
1: MKKGITKRRS RRSKWLVSYL AKLLAPIW TSGGLRASAICA
2: MTTRNRTSKK WRKSGALIKT LQPVMSWL TGGGLRASAICA
3: MKKTRKSAKP RRYMHMLRTW MSVLRDML TSGGLRASAICA
4: MKRRMTKQKK TDKPRRRTRW LRNWLEQW SSAVCVHPLFAP
5: MKKKRKYIRV TLPLSQLNRI WRNVMLQW TSGGLRASAICA

6: MKMMKRKRIS LNQILRDWWR KTGSGVSR QWRSACIRYLR
8: MSNSYRKNNR PRHLRGLPRR LVDLARLV AVCVHPLFAP          (2)
9: MKRTSSSRAS SRRRDAPLLG GLLARLVH QWRSACIRYLR
10:MMKLNKRRRR NRWVSKVVKE WTAYLLPM TVCVHPLFAP

11:MRMKKFRKER QAKRTPWVLP FLKHLAEL TSAGLRASAICA
12:MQKNKNRFKR ASKKEGRRLV VTMLKNFL TAVCVHPLFAP
13:MKSRYKKTRS TRGRYREAFE HAYHTITR LVAVCVHPLFAP
14:MEKKLKKFKQ RRQRFSQLLQ LIRTIIRA TSGGLRASAICA
15:MMPKKWKPSK KRARRRPIQS LLEWVAGA LVAVCVHPLFAP

16:           MRKRQWLDKR DYLVWLLD TMRSACIRYLR
17:MNRRTKSGRL RPRLLRTFMA FMNSLIEM TSGGLRASAICA
19:MSIKFVRRLH ALSKKNYQRV WTKLHERL TSGGLRASAICA
20:MKYKKLNARK FLRALRSALE RYRARVWS TSDGLRASAICA       (2)

21:MSQRKKLLLR RSKRENSRGT LLRAIYNA LVAVCVHPLFAP
22:MIKKKSVGRL RNKLPMFQLF SRLVRKLL TSGGLRASAICA
23:MMKRTKQRKK MVTAARQFLM SWLRQVMQ TSGGLRASAICA
25:MTKRGSKKKL MKKRQWLDKR DYLVWLLD TMRSACIRYLR

26:MNYTKPKKRR TSRKGYLASI WRSYLKWM TSGGLRASAICA
27:MNYKRRKRLN RELAVRKSLY ANVLRALS TWRSGCIRYLR
28:MKKIRSLGKS QLNTLRRLFS RLLRRKML TSSGLRASAICA
29:MSRSSATPRK RGKKKMLRSI MSALRKWL TSSGLRASAICA
30:MKKNTKRKKH AKYVHFVQRA RELLYYAL TSGGLRASAICA
```

Figure B.8. Sequences from round 8. Lysines and arginines are highlighted in red. The numbers in parentheses indicate the number of times (out of 30 clones) that a sequence appears.

Bibliography

Chen, J. L., M. A. Blasco, and C. W. Greider. 2000. Secondary structure of vertebrate telomerase RNA. *Cell* **100**: 503-514.

APPENDIX C:

PROBING THE INTERACTIONS BETWEEN HUMAN TELOMERASE RNA AND THE HUMAN TELOMERASE REVERSE TRANSCRIPTASE RNA-BINDING DOMAIN

This work was done in collaboration with Dr. Peter Snow. This section is dedicated to his memory.

Appendix C

PROBING THE INTERACTIONS BETWEEN HUMAN TELOMERASE RNA AND THE HUMAN TELOMERASE REVERSE TRANSCRIPTASE RNA-BINDING DOMAIN

C.1 Introduction

Maintenance of the ends of eukaryotic chromosomes is performed by the ribonucleoprotein complex, telomerase. Minimally, the telomerase reverse transcriptase (TERT) and the telomerase RNA (TR) are required for the synthesis of the TTAGGG terminal repeats by telomerase. The telomerase reverse transcriptase is composed of unique and variable N- and C- terminal domains that flank a reverse transcriptase (RT)-like domain (reviewed in Autexier and Lue 2006). Human telomerase reverse transcriptase (hTERT) is extremely large (127 kD) and has yet to be effectively overexpressed. Rare codons in the N-terminal region, and folding problems of the intact protein may contribute to the expression difficulties. Through deletion and functional analysis, Lai and co-workers (2001) have identified a 288 amino acid RNA-binding domain in hTERT. This domain is necessary and sufficient for binding to human telomerase RNA (hTR), lies outside the reverse transcriptase motifs, and contains the telomerase-specific "T-motif" (Lai et al. 2001; Nakamura et al. 1997). This appendix describes our efforts to express this RNA-binding domain, and elucidate the complex interactions between hTERT and hTR by finding a minimal hTR that is able to bind the hTERT RNA-binding domain.

C.2 The Human Telomerase Reverse Transcriptase RNA-Binding Domain

Our lab has created a construct for the expression of the hTERT RNA-binding domain (hTERT-288), the sequence between amino acid residues 326 and 613 (hTERT numbering). Using appropriate primers (hTERT288-5: 5'-CCCGGATCCGCCGAGACCCA AGC-3'; and hTERT288-3: 5'-CGTGAATTCTTATCAGTGGTGGTGATCATCGTGCCT GGCTTCCCGATGC-3') the hTERT288 sequence was PCR amplified in a 50 μL reaction containing PCR buffer (10 mM Tris-Cl, pH 9.0; 50 mM KCl, 2 mM $MgCl_2$; 0.1% Triton X-100; 0.2 mM each of dATP, dGTP, dCTP, and dTTP), 40 pmol each primer, 1 ng vector containing the hTERT sequence (generously donated by the Weinberg lab), and 1 μL TAQ. Reactions were heated to 94 °C, followed by 29 cycles of 94 °C for 30 seconds, 60 °C for 1 minute, and 72 °C for three minutes. The PCR product was cleaned via the QiaQuick PCR Purification Kit (Qiagen) and cloned into the pGEX-2T vector (Amersham) using the BamH I and EcoR I sites. We added an N-terminal glutathione-s-transferase (GST) for purification and solubility purposes, as well as a C-terminal histidine (his) tag for purification purposes. In order to accommodate the rare codons found in the hTERT sequence, the vector was transformed into the Rosetta BL21-DE3 line, which supplies rare tRNA codons.

The protein was expressed in *E. coli*. A 5 mL LB + 50 μg/mL ampicillin was grown overnight at 37 °C with shaking. The starter culture was then added to 1 L of fresh LB and allowed to grow at 37 °C with shaking for ~2 hours or until the OD_{600} reached ~0.5. IPTG (1 mM final concentration) was added for induction of protein expression. The protein was expressed at 37 °C for 4 hours with shaking. While expression in *E. coli* was successful, the resulting protein was insoluble. Strategies to increase solubility, by utilizing an N-terminal

ubiquitin tag or inducing slower expression by reducing the temperature from 37 to 30 °C and using less IPTG, were generally unsuccessful in producing soluble protein. Denaturing purification followed by refolding was also unsuccessful in producing a functional hTERT-288.

We then decided to express hTERT-288 in insect cells, since this approach has proven successful in producing purified hTERT with *in vitro* activity (Masutomi et al. 2000; Mikuni et al. 2002). The protein expression was performed by Dr. Peter Snow (Caltech Protein Expression Center) according to established protocols (Masutomi et al. 2000; Mikuni et al. 2002) using the Baculovirus Expression Vector System. The protein was purified via the GST tag under native conditions. The cells were lysed by resuspending the cell pellet in 20 mM Tris-Cl, pH 8.0, 100 mM NaCl, 1% NP-40, 5 mM EDTA, and protease inhibitors (Roche) followed by sonication on ice. The lysed cells were spun down and the lysate applied to a prewashed GST column. The protein was washed with ten column volumes of lysis buffer followed by washing with thirty column volumes of 20 mM Tris-Cl, pH 8.0, and 100 mM NaCl. The protein was then eluted in 50 mM Tris-Cl, pH 8.0, and 20 mM glutathione. Since GST is expressed in the insect cells, endogenous GST was purified from the lysate along with the hTERT-288 construct (figure C.1). Efforts to utilize the His tag for a second purification step were unsuccessful, possibly due to conformational constraints that make the tag inaccessible in the native protein (data not shown). The GST and His tags were not cleaved since the amount of soluble protein purified via the GST tag was low, and further cleavage and purification steps led to an amount of protein insufficient for biochemical analysis.

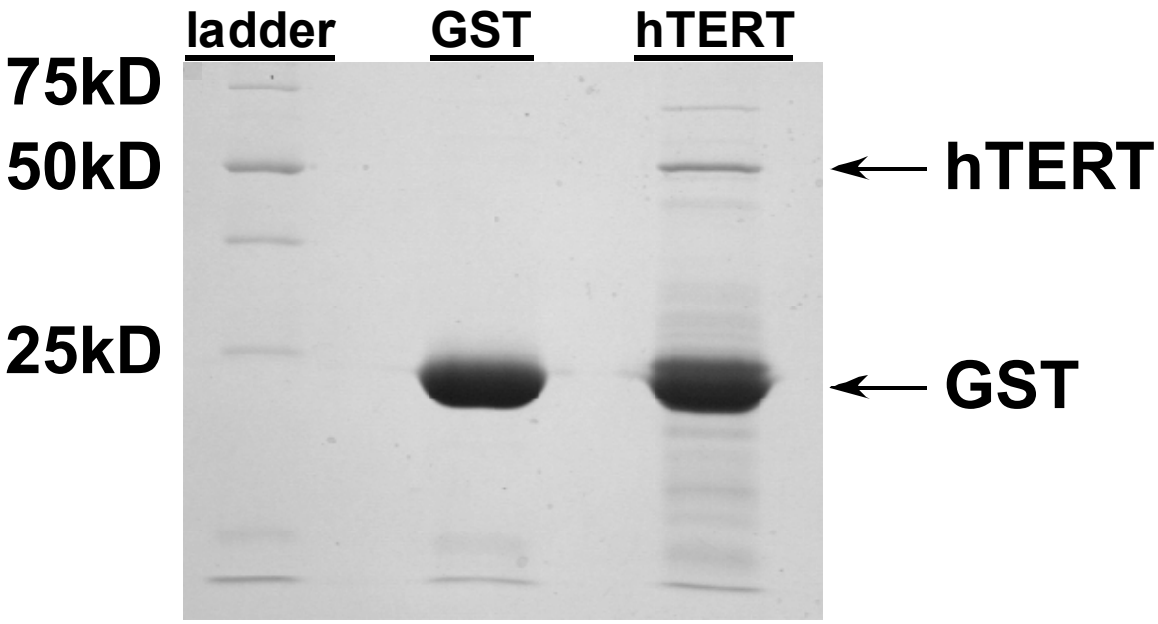

Figure C.1. SDS-PAGE gel of the hTERT-288 protein, purified by the GST tag. hTERT-288 was expressed as a GST fusion, resulting in a protein that is ~55 kD.

C.3 Mobility-Shift Assay between the hTERT-288 Protein and hTR

Preliminary results indicate that the hTERT-288 construct binds to several hTR constructs. The constructs were constructed in a manner similar to the construction of RNA33-147 from chapter 2. Using appropriate PCR primers, RNA208-451, RNA163-330, RNA208-330, and RNA208-360 were PCR amplified in 100 μL reactions from a pUC19 vector containing the DNA sequence encoding for hTR-451 (the complete wild-type hTR sequence). The PCR products were phenol extracted, ethanol precipitated, and digested with BsmB I to cut the vector and generate appropriate ends for run-off transcription. The DNA was then phenol extracted, ethanol precipitated, and dried to pellets. The pellets were then used in 1 mL transcriptions using T7 RNA polymerase. The RNA was gel purified, electroeluted into 0.5X TBE, and ethanol precipitated. The resulting pellets were resuspended in ddH_20 and the concentrations determined by UV spectroscopy and the biopolymer calculator developed by the Schepartz lab (Palmer 1998).

Mobility-shift experiments were performed using the partially purified hTERT-288 construct (figure C.2; figure C.3). The reactions contained 5 nM ^{32}P-end labeled RNA, 0.2 μg or 1 μg hTERT-288, 10 mM Tris-Cl, pH 8.0, 1 mM DTT, 50 mM NaCl, and 10% glycerol. The reactions were assembled without the protein, annealed at 90 °C for 90 seconds and set on ice for two minutes. After addition of protein, the reactions were allowed to sit on ice for 30 minutes before loading to a 6% native gel run in 0.5X TBE at 4 °C. The gel was run at 2W for 2 hours and 40 minutes, dried, and exposed to a PhosphorImager screen. The screen was scanned on a Storm860, and the data analyzed by ImageQuant.

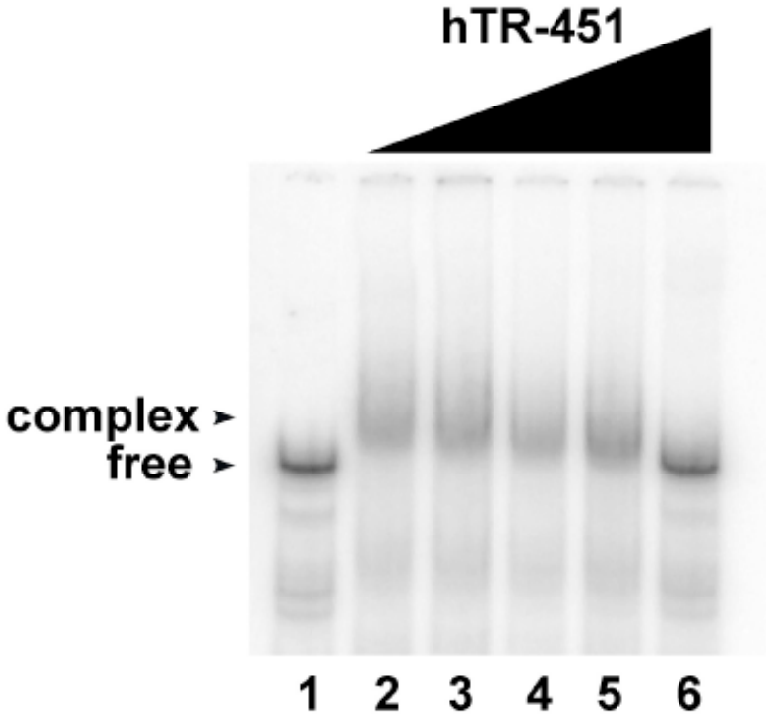

Figure C.2. Competition binding assay between RNA208-451 and increasing concentrations of hTR-451 shows that RNA208-451 and hTR-451 bind to the hTERT RNA-binding domain in a similar manner. Each lane contains 5 nM RNA208-451 and varying concentrations of hTR-451. Lanes 2-6 contain 0.2 μg hTERT-288 protein. Lane 2=no hTR-451; lane 3=5 nM hTR-451; lane 4=25 nM hTR-451; lane 5=50 nM hTR-451; lane 6=500 nM hTR-451.

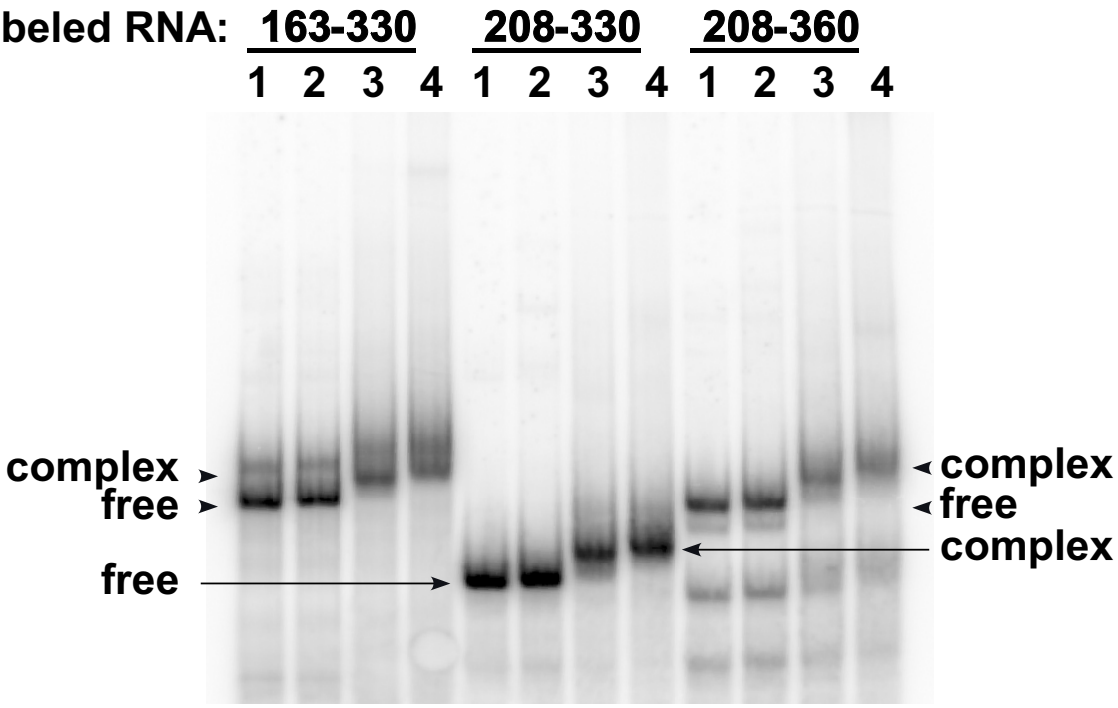

Figure C.3. Mobility-shift assay between hTERT-288 and three hTR constructs. The labeled RNAs (RNA160-330, RNA208-330, and RNA208-360) are CR4/CR5-containing constructs. 1=no protein; 2=GST only; 3=0.2 μg hTERT-288; 4=1 μg hTERT-288. RNA208-330 is sufficient for binding to the hTERT RNA-binding domain.

The hTERT-288 protein displays the ability to bind functionally important regions of hTR. All the constructs tested contain the catalytically critical CR4/CR5 domain. RNA208-451 shifts in the presence of hTERT-288 and can be competed off by hTR-451 (figure C.2). Using the mobility-shift assay, the approximate K_d of the interaction between RNA208-451 and hTERT-288 is 2 μM (data not shown). This value is on the order of previously reported values for association of hTERT and hTR (Xia et al. 2000). As figure C.3 shows, GST does not result in a shift of the labeled RNAs, indicating that the GST tag is likely not participating in the interaction with the RNAs. The data also show that RNA163-330, RNA208-360, and RNA208-330 shift in the presence of hTERT-288 indicating RNA208-330 is sufficient for binding to the RNA-binding domain of hTERT.

Though these results are preliminary, the 123 nucleotide RNA/288 amino acid protein association presented here is a much smaller system compared to the wild-type 451-nucleotide hTR/1132 amino acid hTERT association. A smaller system may be more amenable to future biochemical and biophysical analysis. Additionally, hTERT-288 can be utilized in RNA selection experiments that involve constructing a library of random nucleotides to isolate sequences that bind with high affinity to the hTERT RNA-binding domain. The resulting RNA ligands will provide information about the structural and sequence requirements of hTERT for its RNA partner as well as potentially provide leads for the development of anticancer therapies.

Bibliography

Autexier, C. and N. F. Lue. 2006. The structure and function of telomerase reverse transcriptase. *Annu. Rev. Biochem.* **75**: 493-517.

Lai, C. K., J. R. Mitchell, and K. Collins. 2001. RNA binding domain of telomerase reverse transcriptase. *Mol. Cell Biol.* **21**: 990-1000.

Masutomi, K., S. Kaneko, N. Hayashi, T. Yamashita, Y. Shirota, K. Kobayashi, and S. Murakami. 2000. Telomerase activity reconstituted *in vitro* with purified human telomerase reverse transcriptase and human telomerase RNA component. *J. Biol. Chem.* **275**: 22568-22573.

Mikuni, O., J. B. Trager, H. Ackerly, S. L. Weinrich, A. Asai, Y. Yamashita, T. Mizukami, and H. Anazawa. 2002. Reconstitution of telomerase activity utilizing human catalytic subunit expressed in insect cells. *Biochem. Biophys. Res. Commun.* **298**: 144-150.

Nakamura, T. M., G. B. Morin, K. B. Chapman, S. L. Weinrich, W. H. Andrews, J. Lingner, C. B. Harley, and T. R. Cech. 1997. Telomerase catalytic subunit homologs from fission yeast and human. *Science* **277**: 955-959.

Palmer, C. R. 1998. *Biopolymer Calculator.* Available at http://paris.chem.yale.edu/extinct.html, accessed on September 17, 2003.

Xia, J., Y. Peng, S. Mian, and N. F. Lue. 2000. Identification of functionally important domains in the N-terminal region of telomerase reverse transcriptase. *Mol. Cell Biol.* **20**: 5196-5207.